INNOVATION

ORIGINAL RESEARCH ARTICLE

Orthopedic Effect of Dynamic Loading on Condylar Cartilage

Teixeira CC [a], Abdullah F [b,c], Alikhani M [b], Alansari S [b], Sangsuwon C [b], Oliveira SP [b,d], Nervina JM [b], Wang H [c], Alikhani M [b,e]

a *Department of Orthodontics, New York University College of Dentistry, New York, New York*

b *CTOR Academy, Hoboken, New Jersey*

c *Department of Biomedical Engineering, Stevens Institute of Technology, Hoboken, New Jersey*

d *Department of Mechanical Engineering, Polytechnic Institute of Viseu, Viseu, Portugal*

e *Advanced Graduate Education Program in Orthodontics, Department of Developmental Biology, Harvard School of Dental Medicine, Boston, Massachusetts*

Corresponding Author:
Cristina Teixeira,
Department of Orthodontics
New York University
345 East 24th Street
New York, NY 10010
cristina.teixeira@nyu.edu

Citation: *Teixeira CC, Abdullah F, Alikhani M, Alansari S, Sangsuwon C, Oliveira SP, Nervina JM, Wang H, Alikhani M. Orthopedic Effect of Dynamic Loading on Condylar Cartilage. Innovation. June 2022. 1(4):e1. doi:10.30771/2022.2*

Submitted April 8, 2022
Accepted May 9, 2022

Keywords: *Dynamic loading, condyle, osteogenic effect, chondrocyte proliferation and maturation, condylar growth*

ABSTRACT

Background: We have previously shown that low-magnitude, high-frequency dynamic loading has an osteogenic effect on alveolar bone. Chondrocytes and osteoblasts originate from the same progenitor cells; therefore, dynamic loading may stimulate a similar response in chondrocytes. This could be beneficial for patients with damaged condylar cartilage or mandibular deficiency.

Methods: In vitro studies were conducted using a well described cultured chondrocyte differentiation model. When embryonic chick upper sternum (US) and lower sternum (LS) chondrocytes were treated with retinoic acid and ascorbic acid in culture, only US cells responded to these agents by undergoing differentiation characterized by Type X collagen expression and increased alkaline phosphatase activity. After confluency, chondrocytes were exposed to dynamic load (60 Hz, 0.3 g acceleration, 20 μm amplitude) 5 minutes per day for 5 days, in the presence or absence of retinoic acid (0 and 35nM). The effect of dynamic load on cell proliferation, differentiation and survival was studied at the end of the experimental period. In vivo studies were conducted on growing Sprague-Dawley rats divided into 3 groups: control, static load and dynamic load. Dynamic load was applied 5 minutes per day on the lower right molars at 0.3g acceleration and peak strain of 30 με registered by accelerometer and strain gauge. The static group received an equivalent magnitude of static force (30 με). The Control group did not receive any treatment. Samples were collected at 0, 28 and 56 days for RT-PCR analysis, micro-CT, histology and fluorescent microscopy analysis.

Results: In vitro dynamic loading stimulated the proliferation of US and LS chondrocytes; however, it only enhanced maturation of US chondrocytes. No cellular toxicity was observed. In vivo experiments showed that dynamic loading had a striking effect on condylar cartilage, increasing the proliferation and differentiation of mesenchymal cells into chondrocytes. This effect was accompanied with increased endochondral bone formation resulting in lengthening of the condylar process.

Conclusion: Low-magnitude, high-frequency dynamic loading can positively effect chondrogenesis and endochondral bone formation, both in vitro and in vivo. This effect has the potential to be used as treatment for regenerating condylar cartilage and to enhance the effect of orthopedic appliances on mandibular growth.

Introduction

Primary cartilage and articular cartilage responses to mechanical stimulation have been investigated comprehensively; however, studies on secondary cartilage responses to mechanical stimulation are limited [1-3]. Depending on the type of cartilage and the magnitude and type of mechanical stimulation, cartilage responses can vary significantly. Therefore, results of studies on articular and primary cartilages cannot simply be extrapolated to predict how secondary cartilage reacts to mechanical stimulation. Secondary cartilage evolved to be responsive to its mechanical environment [4-6]. This adaptability shares some features of both primary cartilage and bone. Mandibular condylar cartilage is a secondary cartilage, and it expresses this unique characteristic and adaptability [7, 8].

As an articulating component of the temporomandibular joint, the mandibular condylar cartilage is exposed to a complex and dynamic mechanical environment resulting from oral cavity and craniofacial musculo-skeletal functions. In addition, the mandibular condyle needs to gradually adapt to mechanical challenges induced by the gradual change in position of the mandible in response to soft tissue growth [9-11]. In this regard, mechanical stimulation can be considered the main homeostatic factor for condylar cartilage [1, 12]. However, while loading in the physiologic range may be considered healthy for condylar cartilage growth and function, high- or low- magnitude load could prevent cartilage remodeling or even promote cartilage degradation [13-18].

How condylar cartilage recognizes mechanical stimulation is not clear. Different aspects of mechanical stimulation, such as magnitude, frequency and acceleration of applied load, can target different components of cartilage. In bone, for example, the magnitude and frequency of applied load can cause matrix deformation, which indirectly can be detected by the osteocytes and osteoblasts, while acceleration can be detected directly by these cells [19-23]. While the direction of the applied load (compression versus tension) may affect the anabolic activity as long as it is applied physiologically, it is not the main factor defining the response to mechanical stimulation since both compression and tension can stimulate anabolic activity in cartilage and bone [1, 24-26].

Understanding which component of mechanical stimulation is anabolic for cartilage has considerable therapeutic potential. This is important not only from the standpoint of regenerating damaged condylar cartilage due to conditions such as osteoarthritis, but also as a stimulating factor during orthopedic treatment of mandibular deficiency.

Applying low-magnitude, high-frequency dynamic loads has anabolic effects on weight-bearing bones [21, 27, 28]. Similarly, if this stimulation is applied locally it has anabolic effects on non-weight bearing bones [29, 30]. Considering that condylar cartilage is a secondary cartilage that in many aspects responds to mechanical stimulation similarly to bone, and considering that condylar chondrocytes originate from osteo-chondroprogenitor cells [31], one would expect to observe a similar anabolic response by condylar cartilage. To test this hypothesis, the effect of local application of low-magnitude, high-frequency loading on the mandibular condyle was tested *in vivo* on the mandibular condyle. The specificity of the results was confirmed by in vitro studies using similar stimulation and two different types of chondrocytes.

Materials and Methods

Chondrocyte culture

Upper sternum (US) and lower sternum (LS) chondrocytes were isolated from the sterna of 14-day old chicken embryos, according to the method described previously [32]. Briefly, freshly isolated chondrocytes were plated in 100 mm tissue culture dishes and allowed to proliferate at 37°C and 5% CO_2 in 10 ml complete medium (DMEM; Corning, Manassas, VA, USA) containing 10% Nu serum (Corning, Bedford, MA, USA) and 100 U/ml penicillin/ streptomycin (Corning, Manassas, VA, USA). Chondrocytes were re-plated onto 24-well plates (125,000 chondrocytes/well) and 35mm dishes (350,000 cells/dish), and cultured for an additional 10 days. During the last 5 days, the wells were treated with 35 nM retinoic acid (RA) or vehicle, according to Oliveira et al [33]. In parallel experiments, cells received 35 nM RA or vehicle and a dynamic load as described below. Eighteen days after isolation, cells were collected for different analyses.

Dynamic Loading Device Calibration

The dynamic loading device was prepared and calibrated to deliver a total resultant of 0.3g gravitational acceleration at 60 Hz frequency with a total displacement of 20 μm (Mechanical Engineering Department of the Polytechnic Institute of Viseu, Portugal). The dynamic loading was applied under light-force conditions, since any force above 1000g can decrease the transmissibility of the mechanical stimulation. Under light-force application the device induced a relatively unconstrained motion in vitro. This mechanical stimulation registered a stress of 42 με on cell culture plates. Appliance calibration was performed with a sensor (OMRON-E2E-X7D1-N 23304; OMRON Electronics Iberia SAU, Lisbon, Portugal) that was connected to an oscilloscope (Metrix OX 803B 40 MHz, Metrix Electronics, Hampshire, United Kingdom) and a Digital Tachometer (Lutron DT 2236, Lutron Electronic Enterprise, Taipei, Taiwan).

Application of low-magnitude dynamic loading to cultured cells

Cultured US and LS chondrocytes were subjected to dynamic loading generated by a device that produced 0.3g acceleration and 60 Hz frequency for 5 min per day, as previously described [34]. This acceleration and frequency were selected based on our previous studies that demonstrated their osteogenic effect [29]. The device was sandwiched between two empty 12-well

tissue culture plates and the 12-well plate containing the cells (experimental group or Control group). Two elastic bands prevented the dynamic load from being transmitted to the countertop (and changing the inertial mass of the setup) and vertically secured the 3 layers to each other. Immediately prior to treatment, cells were taken out from the incubator. Control cells were handled identical to experimental cells using the same setup, while the device that produced the dynamic load was not turned on. Treatment was applied at room temperature. After application of dynamic load, cells were returned to the incubator. While outside the incubator, cells from all groups were exposed to room temperature for the same period of time.

DNA quantification

Total DNA quantification was measured using Abcam kit ab156902 (Abcam 156902, Cambridge, MA, US) according to the procedure described by Teixeira et al [35]. Briefly, medium was removed and cells were treated with 0.3 ml 2% Triton X in PBST (Sigma Chemicals, St. Louis, MO). The triton-treated cells were transferred to an Eppendorf tube and frozen at -20°C. The triton extracts/supernatants were then used for DNA quantification. Both the DNA standards and DNA samples (triton extract/supernatant) were prepared in duplicates for quantification. Florescence was measured at 485/20 nm excitation and 528/20 nm emission wavelengths, using Synergy LX Multi-Mode Reader. The results were extrapolated from a standard curve using salmon testis DNA (Sigma-Aldrich) as described previously [32].

ALP activity and staining

ALP activity was measured by a colorimetric assay using an Alkaline Phosphatase Substrate Kit (Bio-Rad 172-1063, Hercules, CA) and measurements were performed as described previously [32, 36]. Briefly, 20 µL of triton extract/supernatant was mixed with 80 µL of ALP substrate solution. Hydrolysis of p-nitrophenylphosphate was monitored over time and readings were completed at a wavelength of 410 nm, using the Synergy LX Multi-Mode Reader. ALP activity was expressed as nmol of product/min/µg of DNA to account for cell number differences [32]. For ALP staining, the cultures were rinsed twice with saline and incubated with 50mM Tris-HCL, pH 9.5 containing 0.5 mg/ml of Napthol as-bi phosphate and 1 mg/ml of Fast Red trisodium salts (Sigma) for 2 minutes at 37°C. After incubation, the solution was removed, plates were rinsed with saline, air dried and photographed.

Cell cytotoxicity/survival test

Cell cytotoxicity was evaluated using the quantitative colorimetric MTT Cell Proliferation Assay Kit (Cayman Chemical 10009365, Ann Arbor, MI, USA) and measurements were performed as described previously [37]. Briefly, 300 µL of MTT reagent was added to the media of each well, and incubated for 3 hours at 37°C in a CO_2 incubator. After incubation, the media was removed, cells were washed and 100 µL of crystal dissolving solution was added to each well, producing a purple solution. 50 µL of the purple solution was transferred to a 96 well plate and the absorbance was measured at a wavelength of 590 nm, using the Synergy LX Multi-Mode Reader (BioTek, Winnooski, VT, USA) [38-40].

Animals

60 growing male Sprague-Dawley rats (21 days old) with an average weight of 45 gr, were divided into 3 groups: Control, static load and dynamic load groups (Table 1). Dynamic load (0.3g, 60 Hz) was applied 5 minutes per day to the mandibular right molars under 3% isoflurane anesthesia for the duration of the study. The static group received an equivalent magnitude of loading to produce similar strain on the alveolar bone (30 µε) for 5 minutes per day. The Control group did not receive anesthesia or any loading treatment. Samples were collected at 28 and 56 days for histology, RT-PCR analysis, micro-CT and fluorescent microscopy analysis. Three days before euthanasia, 6 animals in each group were given an intraperitoneal injection of bromodeoxyuridine (BrdU, Sigma, St. Louis, MO, USA) at the dosage of 5mg/100 g body weight. The injection was administered to each rat at the same hour of the day. In addition, 4 animals in each group received a calcein green (15 mg/kg, i.p.) injection on days 0 and 25 and were euthanized on day 28. Four animals in each group were euthanized on day 56 for micro-CT and histological studies. Animal protocol approved by New York University Institutional Animal Care and Use Committee (protocol # PROTO201900047).

Table I. Number of animals

Experimental Group	Total number	Age (weeks)	Real-time PCR	MicroCT	Histology	Fluorescent Microscopy
Control	20	3	6 condyles	10 condyles	10 condyles	4 Condyles
Dynamic Load	20	3	6 condyles	10 condyles	10 condyles	4 Condyles
Static Load	20	3	6 condyles	10 condyles	10 condyles	4 Condyles

NOTE: Condyles used for MicroCT were also used for Histology

Calibration of dynamic and static loading in vivo

A strain gauge (UFLK-1-11-1L, 1 mm gauge length, 120 Ω TML Gages, Texas Measurements, College Station, TX, USA) was attached to the buccal side of the alveolar bone near the mandibular third molar on fresh and dry rat skulls using cyanoacrylate. Strain signals were amplified by a low-noise amplifier (SX500, Beacon Dynamics, Byram Township, NJ, USA). Data acquisition and analyses were performed with the SPIDER 8 system and Catman 4.5 software measured with a piezoelectric sensor-Bimorph vibration element 4V5mm (Allied Electronics, Fort Worth, TX, USA), and a MotionNode 3-DOF inertial measurement unit (GLI Interactive, Seattle, WA, USA). Dynamic load produced a very low peak strain of 30 µε (microstrain), measured at the buccal alveolar bone surrounding the mandibular molars by the strain gauge (Figure 3A).

Micro-computerized tomography (MicroCT) and bone morphometric analysis

Mandibles were scanned in a Scanco MicroCT (μCT40, Scanco Medical AG, Bassersdorf, Switzerland). The bones were scanned at an energy of 70kV and intensity of 114mA, with 300 ms integration time, resulting in 16-mm isotropic voxel size. Results were analyzed utilizing μCT V6.0 software on the HP open platform (OpenVMS Alpha Version 1.3-1 session manager). The scanned area of interest included the condylar, coronoid and angular processes of the mandible (Figure 3B). The Region of Interest (ROI; Figure 3C purple box) on the condylar process was delimited by the following planes: 1) Inferior plane (Plane A): a plane passing through the apex of the superior mandibular notch and the inferior mandibular notch; 2) Superior plane (Plane B): a horizontal plane parallel to the inferior plane that is tangent to the condyle apex; 3) Mesial plane: a vertical plane perpendicular to inferior plane and tangent to the mesial surface of the condyle; 4) Distal plane: a vertical plane perpendicular to the inferior plane and tangent to the distal surface of the condyle. The ROI was then rotated to the coronal view for histomorphometry measurements. Specifically, bone parameters were measured in a rectangular area confined between the cortical bones mesio-distally and inferior-superiorly (approximately 4.3 x 1.5 mm). Morphometric measurements taken were: 1) trabecular bone volume fraction (BV/TV%), 2) trabecular thicknesses (Tb. Th.), 3) trabecular number (Tb. N.), and 4) trabecular space (Tb. Sp.).

Histology, immunohistochemistry and fluorescence microscopy

Condyles were harvested and fixed in 4% paraformaldehyde, demineralized in 14% EDTA solution for 2 weeks, dehydrated in alcohol series, embedded in paraffin, and cut into 5 μm sections (RM 2265 Leica microtome; Leica Biosystems, Buffalo Grove, IL, USA). Five frontal sections through the middle third of the condyle were stained with hematoxylin and eosin (H&E), five sections were used for BrdU staining and quantification and five sections were used for TRAP straining. Sections of each sample were scanned on a Scan Scope GL series optical microscope (Aperio, Bristol, UK) and analyzed at 20× magnification. For BrdU quantification, sections were immunostained using BrdU staining kit following the manufacturer's instructions (Zymed Laboratories-Invitrogen Corporation, Carlsbad, CA). Negative controls consisted of omitting the primary antibody step and incubating with blocking solution only. For osteoclast identification, sections were immunostained using Vectastin ABC kit (Vectastin ABC kit, Vector Laboratories, Burlingame, CA, USA) with an antibody for tartrate-resistant acid phosphatase (TRAPcP-5b; Zymed antibodies; Invitrogen, Carlsbad, CA, USA), an osteoclast marker. As a negative control, sections were exposed to pre-immune serum.

Sections stained with H&E were used for morphological studies and measurements of the height of the chondroblast and hypertrophic layer. Values were determined as the mean of three sections with measurements performed in the middle third of frontal cuts of the condyle. The number of BrdU-labeled cells within the proliferative layer and in the cell layers underneath it (pre-hypertrophic and hypertrophic) was counted in 3 sections in the middle third of the frontal cuts of the condyle, in a fixed rectangular region under the same magnification, and averaged.

Osteoclasts were defined as TRAcP-5b-positive multinuclear cells at the chondro-osseous border of the cartilage and bone. The mean was calculated from 3 sections in the middle third of frontal cuts of the condyle, in a fixed rectangular region under the same magnification. Two examiners completed all histological quantifications.

For fluorescence microscopy, specimens were fixed in formalin, washed overnight in running water, dehydrated in an alcohol series, cleared with xylene, and embedded in methyl methacrylate. Samples were sectioned at 5-7 μm thickness on an RM 2265 Leica microtome, viewed and photographed through a fluorescent microscope (Nikon Microscopy; NIS Elements Software, Tokyo, Japan).

Mandibular morphological measurements

Mandibular morphological measurements were done on reconstructed images from micro-CT scans. The parameters measured and compared were: 1) Condylar process length (condylion to the anterior border of mandibular foramen) and 2) Condylar head width in the sagittal view (distance from the most anterior to the most posterior point of the condylar articular surface). Each measurement was completed in triplicate and averaged

RNA Analysis

For total RNA extraction, six animals from each group were sacrificed by CO_2 narcosis at 24 hours, and the condyles were dissected and frozen in liquid nitrogen. Total RNA was collected as described previously [41]. Real-time PCR for bone formation and bone resorption markers was performed with primers specific for rat genes, with a QuantiTect SYBR Green RT-PCR kit (Qiagen, Valencia, CA, USA) on a DNA Engine Optican 2 System (MJ Research, Waltham, MA, USA). An mRNA pool for each group was tested three times. Relative levels of mRNA were calculated and normalized to the level of GAPDH and acidic ribosomal protein mRNA.

Statistical analysis

After confirming normal distribution of samples by the Shapiro-Wilk test, group comparisons were assessed by analysis of variance (ANOVA). Pairwise multiple comparison analysis was performed with the Tukey's post hoc test. Two-tailed p values were calculated; $p < 0.05$ was set as the level of statistical significance.

Results

RA induced chondrocyte maturation in vitro

We chose a well-described culture model, extensively used in studies of chondrocyte maturation. Chondrocytes from the upper sternum (US) have the potential to undergo maturation and induce bone formation when implanted in vivo [42, 43]. Chondrocytes from the lower sternum (LS), behave as permanent cartilage cells in vitro and in vivo, and therefore, were used as controls. Our results validated this model by showing that US chondrocytes grown in monolayer for 1 week underwent maturation in a dose-dependent manner when treated with 0 – 100 nM RA (Figure 1, upper wells). However, LS chondrocytes did not respond to RA treatment at any concentration (Figure 1, lower wells). Since we observed a significant increase in ALP staining at 35 nM RA, we performed the remainder of our *in vitro* experiments using this concentration.

Dynamic loading mimics RA-induced increased chondrocyte proliferation, survival and maturation

To evaluate the effect of low-magnitude, high-frequency dynamic loading on chondrocyte proliferation, survival and maturation in vitro, cell cultures were exposed to a dynamic or static load 5 min per day, for 5 days in the absence or presence of RA.

Chondrocyte proliferation was assayed by DNA concentration in the cells (Figure 2A). In the absence of RA, no difference was observed between the proliferation of US and LS cells exposed to static load ($p > 0.05$). The presence of 35 nM RA significantly increased the proliferation of LS cells 2.2-fold ($p < 0.05$), while US showed a modest, non-significant 1.5-fold increase in proliferation ($p > 0.05$). Dynamic loading in the absence of RA increased the proliferation of LS cells 2.1-fold ($p < 0.05$), but only stimulated a slight increase of 1.6-fold in proliferation of US cells ($p > 0.05$). When chondrocytes were exposed to dynamic loading in the presence of 35nM RA there was a statistically significant increase in the proliferation of both LS and US chondrocytes 4.8- and 2.8- fold, respectively, ($p < 0.01$). Interestingly, when we compared the combined effect of dynamic loading and RA with the effect of RA alone, we observed a 2.1-fold increase in LS cell proliferation and 1.9-fold increase in US cell proliferation, and both were statistically significant ($p < 0.05$). As demonstrated in Figure 2A, low-magnitude, high-frequency dynamic loading mimics the proliferation effect of 35 nM RA on LS and US chondrocytes. Equally important, RA and dynamic loading acted synergistically to significantly increase LS and US chondrocyte proliferation, with the effect being more dramatic in LS chondrocytes.

ALP activity is an important marker of hypertrophy and maturation of chondrocytes. We first measured ALP activity in the absence or presence of 35 nM RA (Figure 2B). As expected, RA treatment of LS chondrocytes did not stimulate an increase in ALP activity when compared to vehicle-treated LS cells ($p > 0.05$). However, US chondrocytes showed a statically significant 3.5-fold increase in ALP activity compared to vehicle-treated US cells ($p < 0.01$). Additionally, we observed no difference in ALP activity between LS and US cells in the absence of RA ($p > 0.05$), while 35 nM RA significantly increased ALP activity in US chondrocytes compared to LS chondrocytes ($p > 0.05$).

Next, we investigated the impact of dynamic loading in US and LS maturation. Dynamic loading in the absence of RA did not increase ALP activity in LS cells ($p > 0.05$); however, dynamic loading alone significantly increased ALP activity in US cells 2.3-fold compared to US cells that received static load ($p < 0.01$). We then examined the combined effect of RA and dynamic loading in LS and US chondrocytes. Combining dynamic loading with RA treatment did not significantly increase ALP activity in LS chondrocytes compared to RA treatment alone ($p > 0.05$). On the other hand, US chondrocytes treated with the 35 nM RA showed a significant 1.8-fold increase in ALP activity when exposed to dynamic loading in comparison to static load ($p < 0.05$).

To evaluate how dynamic loading impacts chondrocyte survival in the presence or absence of RA, we conducted an MTT assay (Figure 2C). Small changes in metabolic activity of the cells can generate large changes in MTT, allowing one to detect cell stress in the absence of direct cell death upon exposure to experimental conditions [44].

Our results showed that LS chondrocytes exposed to loading presented a 25% increase in MTT conversion in comparison with cells that received static load, which was statistically significant ($p < 0.05$). In the presence of RA and loading this increase was even more prominent 43% ($p < 0.05$), which demonstrate not only that loading did not induce stress on the cells, it stimulated them to proliferate. US chondrocytes exposed to dynamic load showed a 3% increase in MTT conversion ($p > 0.05$), while in the presence of RA and loading this increase was 26% ($p < 0.05$).

Indirect dynamic loading increased sub-condylar bone density in vivo

Having demonstrated a chondrocyte response to dynamic loading *in vitro*, we wanted to determine if dynamic loading impacts the mandibular condyle *in vivo*. Since we cannot directly apply dynamic force to the condyle, we applied dynamic loading indirectly through the dentition. We have previously demonstrated that indirect delivery of dynamic loading through the molars produces significant changes in mandibular cortical and trabecular bone [29]. Therefore, to verify that our treatment is producing the desired effect, we first examined the dynamic loading on condylar bone. Specifically, we applied a low-magnitude dynamic load (30 με) in the form of high-frequency acceleration (60 Hz, 0.3 peak resultant acceleration, 20 μm displacement) to the right mandibular molars of adult rats, 5 minutes per day for 28 days (Figure 3A). The effect of loading

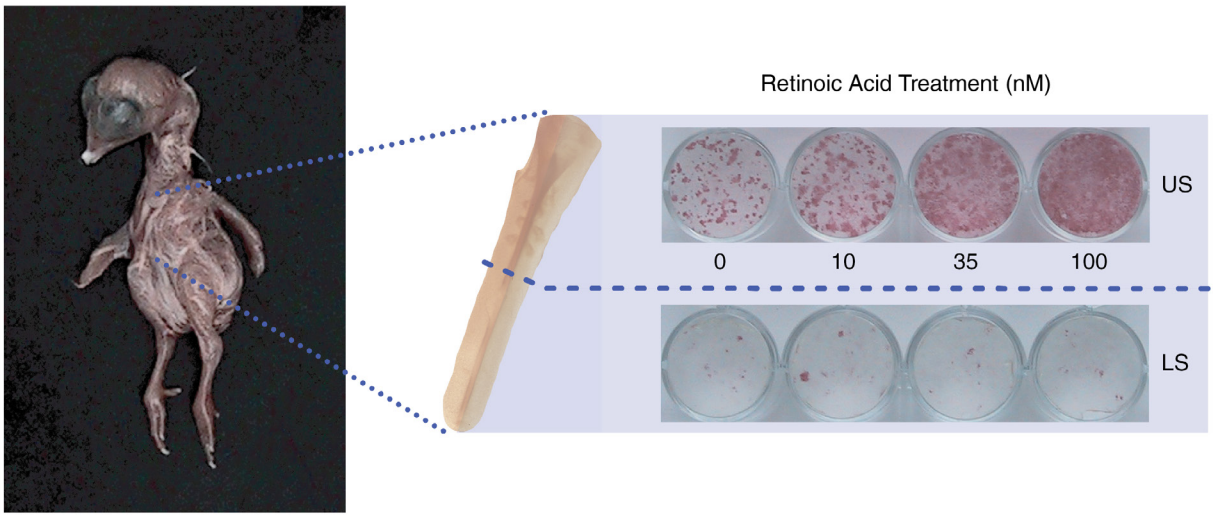

Figure 1: Culture model using embryonic chick chondrocytes. *Chondrocytes were dissected from the upper sternum (US) and lower sternum (LS) of 14-day chick embryos, cultured in monolayer and treated with retinoic acid (RA) at different concentrations (10, 35, and 100 nM) to induce chondrocyte maturation. Photomicrographs of cells show a dose-dependent increase in alkaline phosphatase activity (increase in red color) only on US chondrocytes. LS chondrocytes did not respond to RA nor undergo maturation, and therefore, were used as controls in our studies of maturation-dependent events.*

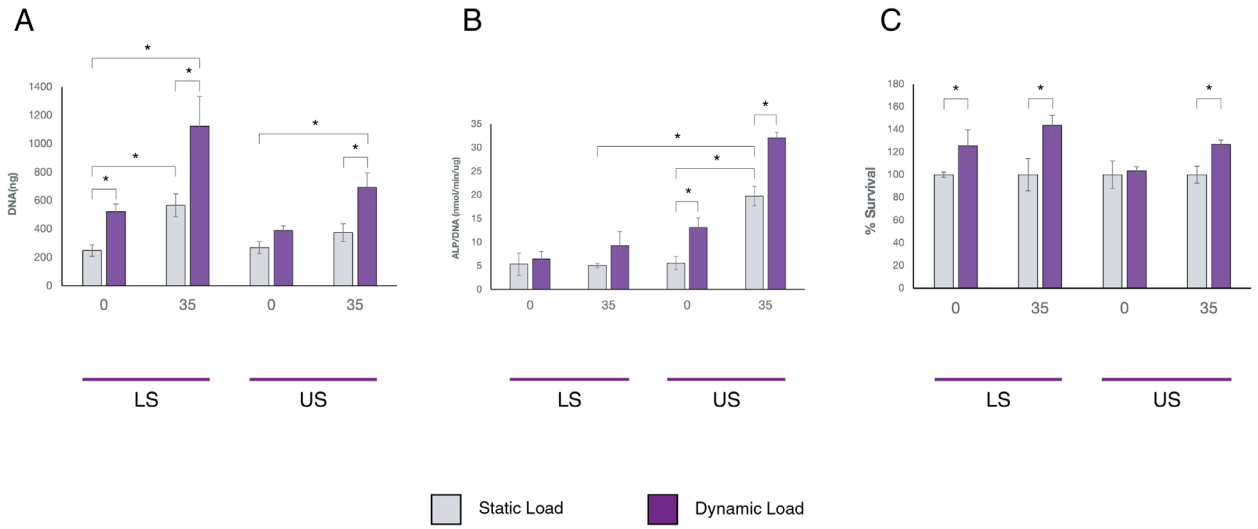

Figure 2: Dynamic loading effect on chondrocyte proliferation, differentiation and survival, in vitro. *To study the effect of dynamic loading on chondrocyte proliferation, cultures isolated from the lower (LS) or upper (US) sternum were treated with 35 nM RA (35) or vehicle (0) in the absence (Static Load) or presence (Dynamic Load) of low-magnitude, high frequency dynamic loading. Dynamic loading was applied every day for 5 minutes. (A) Chondrocytes were harvested after 5 days and DNA concentration was determined. (B) To investigate the effect of dynamic loading on chondrocyte differentiation, alkaline phosphatase activity was measured spectrophotometrically in cell cultures after 5 days, and normalized to the total DNA content of each sample. (C) Chondrocytes survival was measured after 5 days by a quantitative colorimetric assay using MTT Cell Proliferation Assay Kit. Results are presented as percentage of Control (no load) for the same RA concentration. Values represent the mean + SEM of four different experiments with three replicate cultured cells in each group. * Statistically significant differences between groups (p> 0.05).*

on sub-condylar bone density was studied by micro-CT in the Region of Interest (ROI) (Figure 3B and C). After 28 days of dynamic loading the density of the sub-condylar bone increased in comparison with the Control group (Figure 3D).

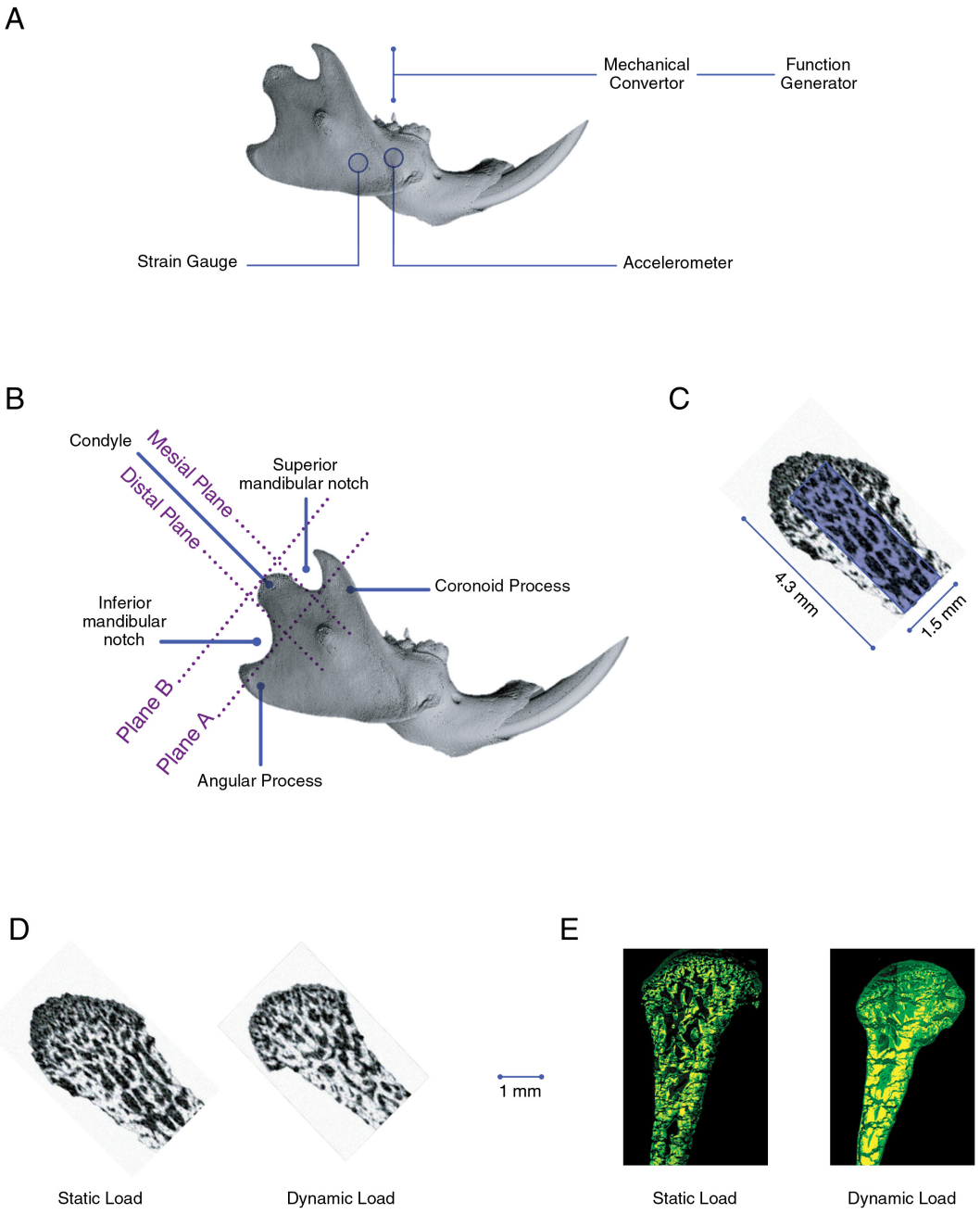

Figure 3: In vivo experimental model shows condyle response to dynamic loading. *A low-magnitude, high-frequency dynamic load (120 Hz, 0.3 peak resultant acceleration, 20 µm displacement and 30 µε) was applied to the lower right molars for 5 minutes per day, for different time periods. (A) Schematic shows the location of the strain gauge and accelerometer that allowed the evaluation of micro-strain and acceleration on the alveolar bone. (B) Region of Interest (ROI) where the condylar bone quantity and quality were evaluated was limited inferiorly by a plane passing through the apex of the superior mandibular notch and inferior mandibular notch (Plane A) and superiorly by a plane parallel to the Inferior plane passing through the apex of the condyle (Plane B). From the mesial and distal side, a plane perpendicular to the inferior plane and tangent to the mesial and distal surfaces of the condyle define the limits of the ROI. (C) Bone parameters were measured in a rectangular area (inside purple rectangle) of approximately 4.3 x 1.5 mm. (D) 3-D reconstructed µCT images of the condylar process of Dynamic Load or Static Load groups collected at 28 days. Note the marked increase in bone density in the Dynamic load group. (E) Fluorescence microscopy images of frontal sections of the condylar process after 28 days of dynamic or static load application. Animals received calcein green (15 mg/kg, i.p.) injections on days 0 and 25 and were euthanized on day 28. Note the significant increase of the osteogenic activity shown as increased fluorescence in Dynamic Load group.*

A quantitative evaluation of sub-condylar bone (Figure 4) demonstrated that indirect dynamic loading significantly increased BV/TV ($p < 0.03$) and BMD ($p < 0.03$). The increased bone formation occurred mostly through increased trabecular thickness ($p < 0.02$) and decreased in trabecular spacing ($p < 0.02$), with trabecular number remaining constant ($p > 0.05$). Interestingly, no significant difference was observed between the group that did not receive any treatment and the Control group that received a static load ($p > 0.05$) (Figure 4).

Sub-condylar BV/TV was significantly higher in animals that were exposed to dynamic loading than in the Static and Control groups at both day 28 ($p < 0.03$) and day 56 ($p < 0.01$) (Figure 5A). While longer application of indirect dynamic load showed higher BV/TV values, the difference between day 28 and day 56 was not statistically significant ($p > 0.05$) (Figure 5A).

The increase in bone density in response to dynamic loading was dependent on the point of load application. To assess this, we examined the effect of static and dynamic loading of the right condyle (close application point) on µCT changes in the left condyle (distant application point) (Figure 5B). The dynamic load group had more bone on the right condyle (close application point) compared to the left condyle (distant application point), although the difference did not reach significance when compared to the static load group ($p > 0.05$; data not shown).

To further verify the osteogenic effect of indirect dynamic loading on mandibular bone, we performed fluorescence microscopy. We found significant osteogenic activity (Figure 3E) in the condyles after 28 days of indirect dynamic loading.

It should be emphasized that local application of dynamic or static load did not have any effect on the weight of the animals and no difference between Control, Static Load and Dynamic Load groups was observed (Table II).

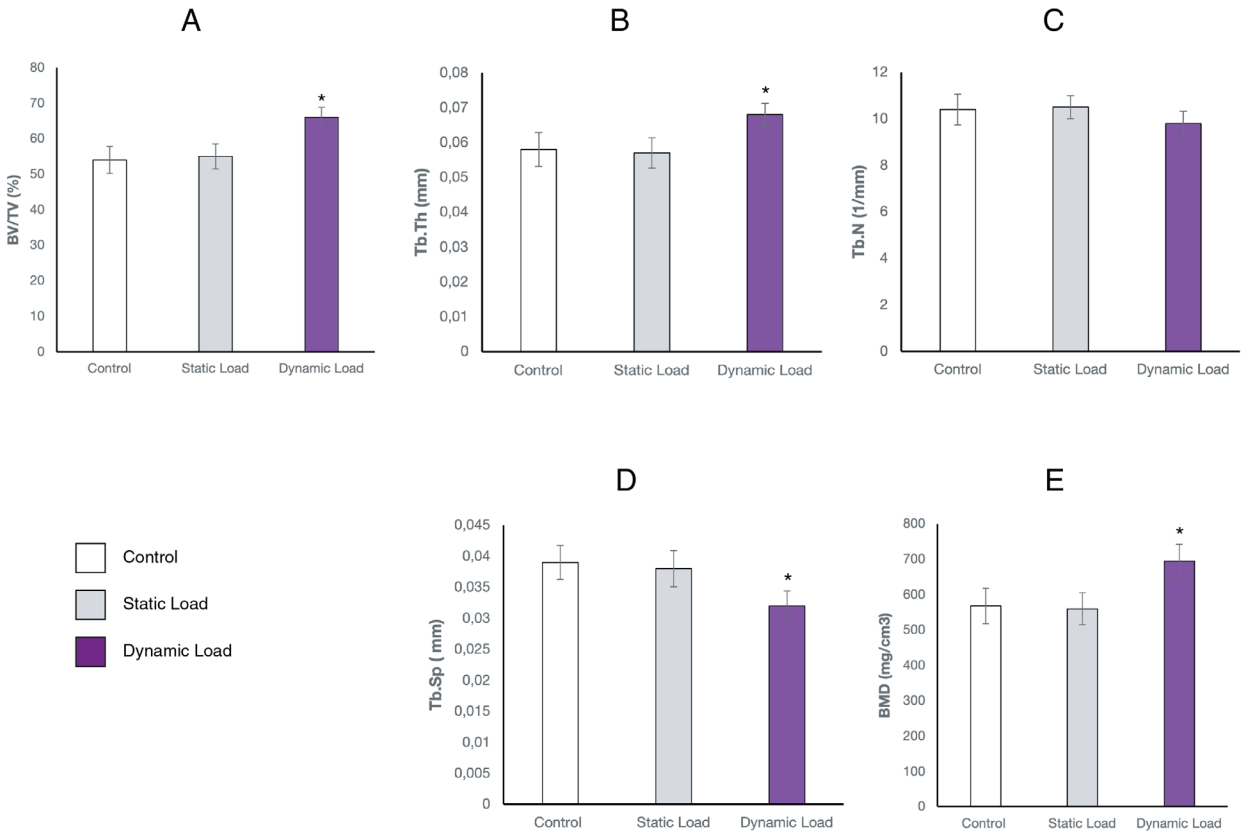

Figure 4: Dynamic loading increased condylar bone volume and density. *Parametric values of condylar bone were determined from uCT data for Control, Static Load and Dynamic Load groups at day 28. Graphs show (A) Bone Volume fraction (BV/TV), (B) Trabecular Thickness (Tb. Th.), (C) Trabecular number (Tb. N.), (D) Trabecular space (Tb. Sp.), and (E) Bone Mineral Density (BMD) of the condylar bone. Each value presents mean ± SEM of 6 samples. * Statistically different from Control and Static groups.*

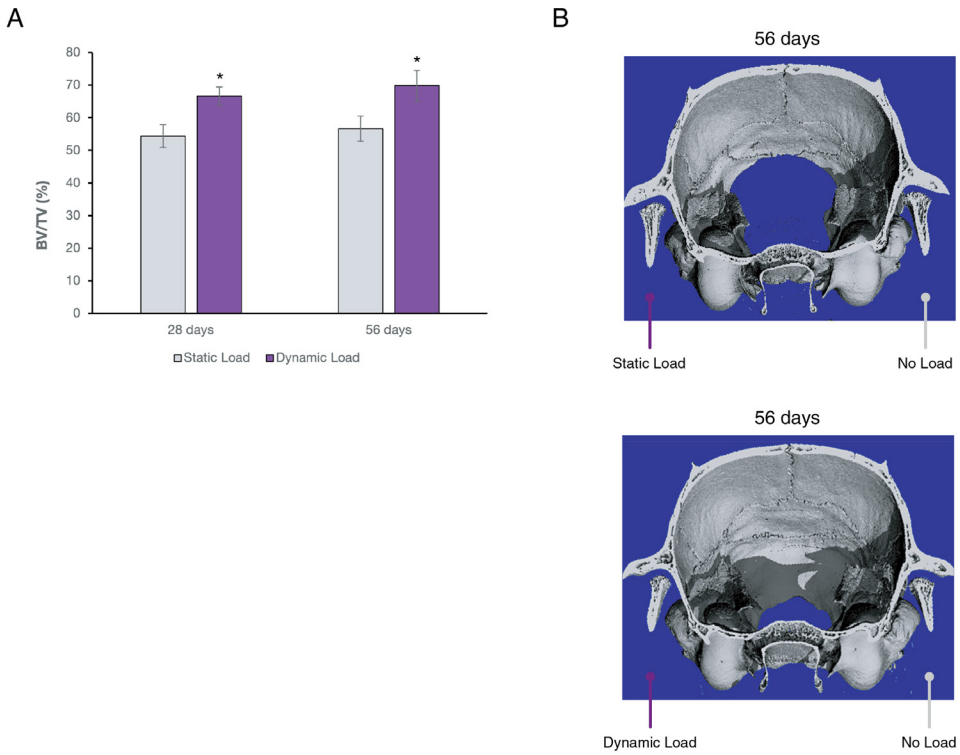

Figure 5: Osteogenic effect reached a plateau and was restricted to the side of load application. *(A) Graph shows Bone Volume fraction (BV/TV) of animals that received static or dynamic load for 28 and 56 days. Each value presents mean ± SEM of 6 samples. * Statistically different from Static Load group. (B) 3D µCT reconstruction of the skull of rats that received dynamic, but not static, load on the right mandibular molars for 56 days show higher bone density in the condylar process closer to source of the load.*

Table II. Effect of dynamic load on body weight.

Experiment Duration	Control	Static Load	Dynamic Load
28 days	223 ±34	219 ± 38	225 ± 31
56 days	359 ± 39	364 ± 27	361 ± 34

NOTE: no statistically significant difference observed between different groups (p >0.05)

Table III. Effect of Dynamic load on condylar dimensions. *Measurements of length, width and percentage of growth in each of dimensions compared to Baseline. Value represents the mean + SEM of 4 animals.*

Experimental Group	Length (mm)	Width (mm)	Percentage growth in length/width (%)
Baseline	6.1 ± 0.4	2.2 ± 0.2	---
Static Load	8.3 ± 0.7*	4.2 ± 0.2*	36 / 90
Dynamic Load	9.2 ± 1.2*#	3.9 ± 0.3*#	51 / 77

* Significantly different from Baseline group; # Significant different from Static Load group (p < 0.05)

Indirect dynamic loading increased condylar process length more than width

Indirect dynamic loading of the mandible caused changes of the mandibular dimensions measured in microCT images (Figure 6A). After 56 days, condylar head length increased 15% in the animals that received dynamic load in comparison with animals that received the static load, which was a statistically significant increase ($p < 0.05$; Figure 6B and Table III). This rapid increase in condylar head length was accompanied with a slower increase in condylar head width, which was 13% narrower in these animals ($p < 0.05$), which demonstrated an increase in the rate of endochondral bone formation and remodeling posteriorly and superiorly. Interestingly, these changes in length and width were not observed on the opposite side of the mandible, which did not receive any mechanical stimulation ($p > 0.05$; data not shown).

The frontal condylar process view in animals that received the dynamic load demonstrated increased curvature of the ramal process compared to animals that received static load (Figure 6C). This curvature was not observed on the contra-lateral side, suggesting a compensatory adaptation of the faster growing side to keep the symmetry and function of the jaws.

Indirect dynamic loading increased chondrocyte proliferation and differentiation/maturation in vivo

Having verified that our indirect dynamic loading model produces predictable morphological, cellular and molecular changes, we wanted to investigate whether these osteogenic changes are associated with changes in the condylar cartilage. To begin, we examined the cellular responses histologically. At the beginning of the experiments (baseline), five clear morphological regions were recognizable in the condylar process: 1) Articular, 2) Proliferative, 3) Pre-Hypertrophic (chondroblast), 4) Hypertrophic and 5) Chondro-osseous junction regions (Figure 7A). Since no differences between Control and Static Load groups was observed, histological sections of Static and Dynamic Load groups are presented for simplicity.

After 28 or 56 days of indirect dynamic loading, a significant difference in the height of the pre-hypertrophic zone was measured compared to the Control and Static Load groups ($p < 0.05$; Figure 7A,B and C). Similarly, 28 or 56 days of indirect dynamic loading, the height of the hypertrophic zone also increased significantly compared to the Control and Static Load groups ($p < 0.05$; Figure 7D). No significant differences were detected between the Static Load groups and Controls in either experiment.

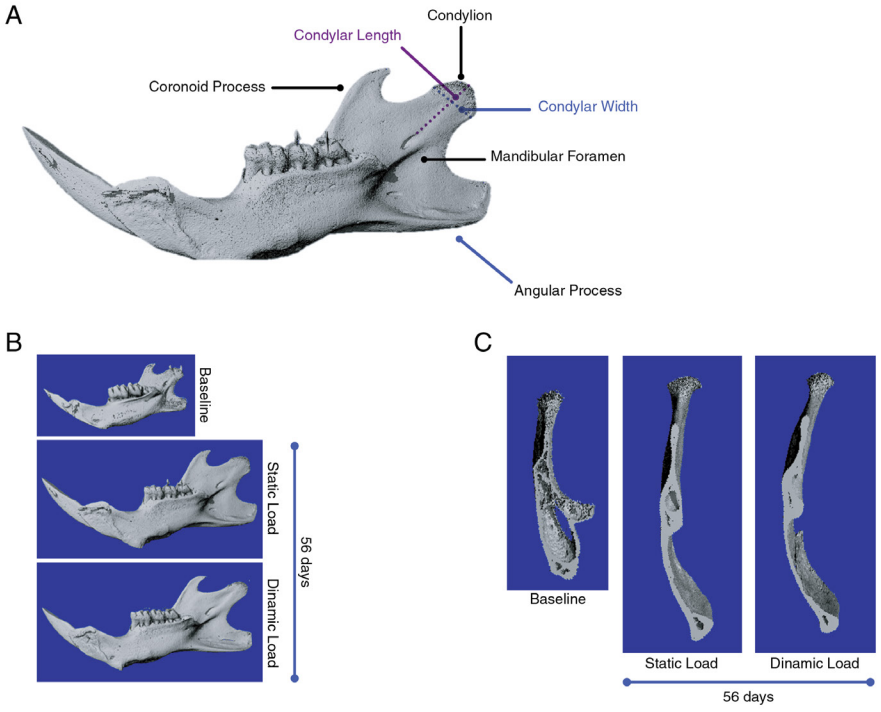

Figure 6: Effect of dynamic loading on condylar length and width. *µCT 3D reconstruction images (A-C) were used to measure the length and width of the condyle, as shown in the schematic. Measurements were performed on mandibular condyles at Baseline (before initiation of experiment), and in Static and Dynamic Load groups at 56 days (D). Dynamic loading caused a significant increase in the length (B) and decrease in the width (C) of the mandibular condyles.*

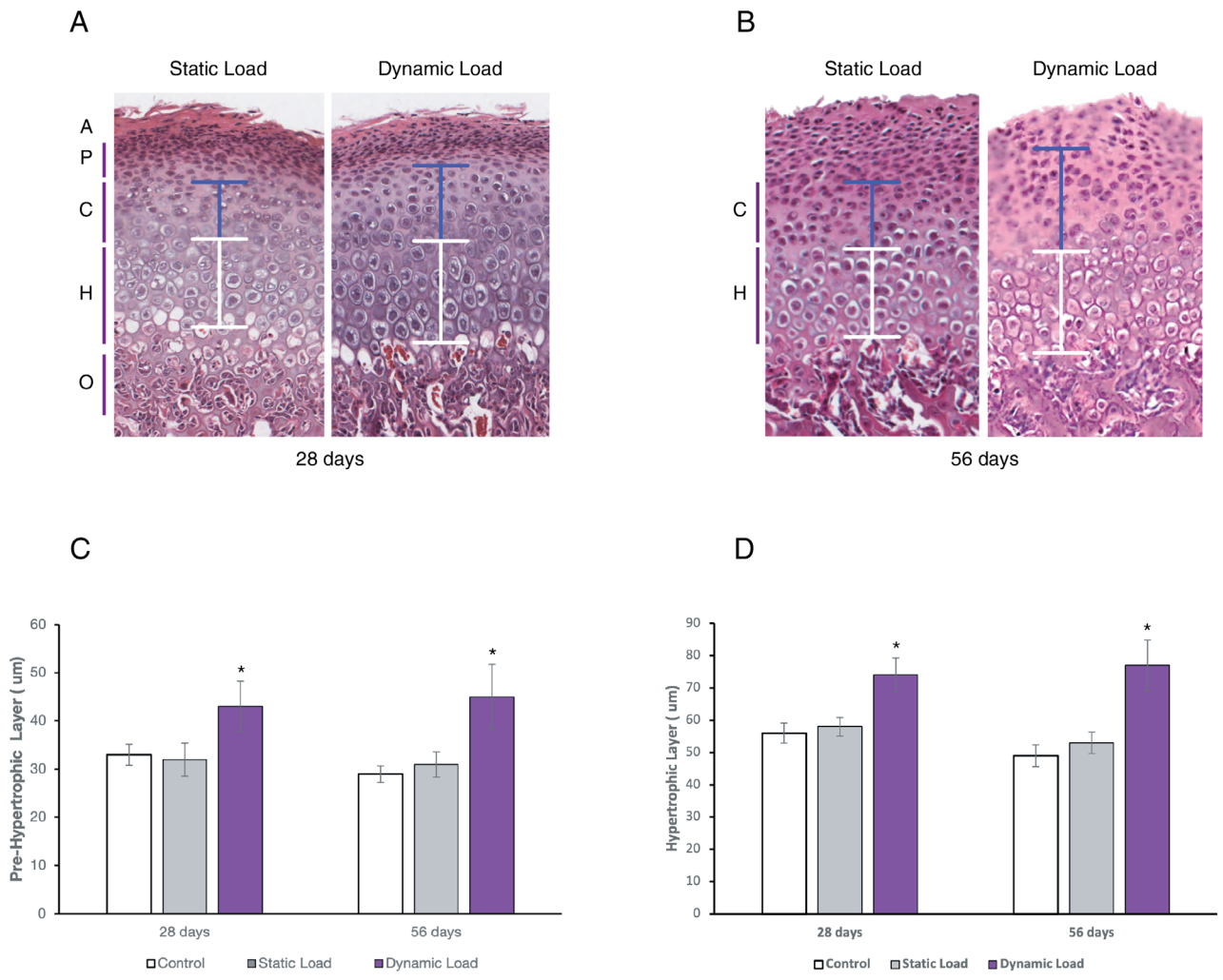

Figure 7: Dynamic loading induces changes in condyle cartilage organization. *Hematoxylin & Eosin stained longitudinal sections through the condylar cartilage and bone show different morphological layers at 28 and 56 days (A, articular zone; P, proliferative zone; C, pre-hypertrophic zone; H, hypertrophic zone; O, chondro-osseous junction). Photomicrographs show the different zones in experimental animals that received static or dynamic loading for 28 days (A) or 56 days (B). The height of the pre-hypertrophic (C) and hypertrophic (D) zones in control animals that went through natural growth and animals that were exposed to 28 days or 56 days of static or dynamic loads were measure in photomicrographs of H&E stained sections. Values are mean ± SEM of 6 animals.*

Injection of BrdU three days before euthanasia at day 28 revealed labeled cells in the proliferative and sub-proliferative zones (pre-hypertrophic and hypertrophic chondrocytes; Figure 8A). Quantification of labeled cells showed that they were present at significantly higher numbers in experimental animals that received indirect dynamic load ($p < 0.05$) (Figure 8B). In addition, the majority of these cells were located in the proliferative zone (56%) in the Static group animals. Interestingly, 48% of these cells were in the proliferative zone and the rest had already migrated to subjacent layers (especially the pre-hypertrophic and upper hypertrophic layers) in the Dynamic Load group.

Having demonstrated that indirect dynamic loading increased the rate of endochondral bone formation, we investigated the number of osteoclasts in the condylar cartilage. We found that at day 28, the number of osteoclasts at the border between cartilage and bone (chondro-osseous border) increased significantly in the Dynamic Load group in comparison with the Static Load group, which was statistically significant ($p < 0.05$; Figure 8C and D).

Indirect dynamic loading increased expression of chondrogenic and osteogenic markers

To further study the effect of dynamic loading on cartilage and bone, and the process of endochondral bone formation, expression of different transcription factors, cartilage markers and bone markers were studied by real time RT-PCR (Figure 9).

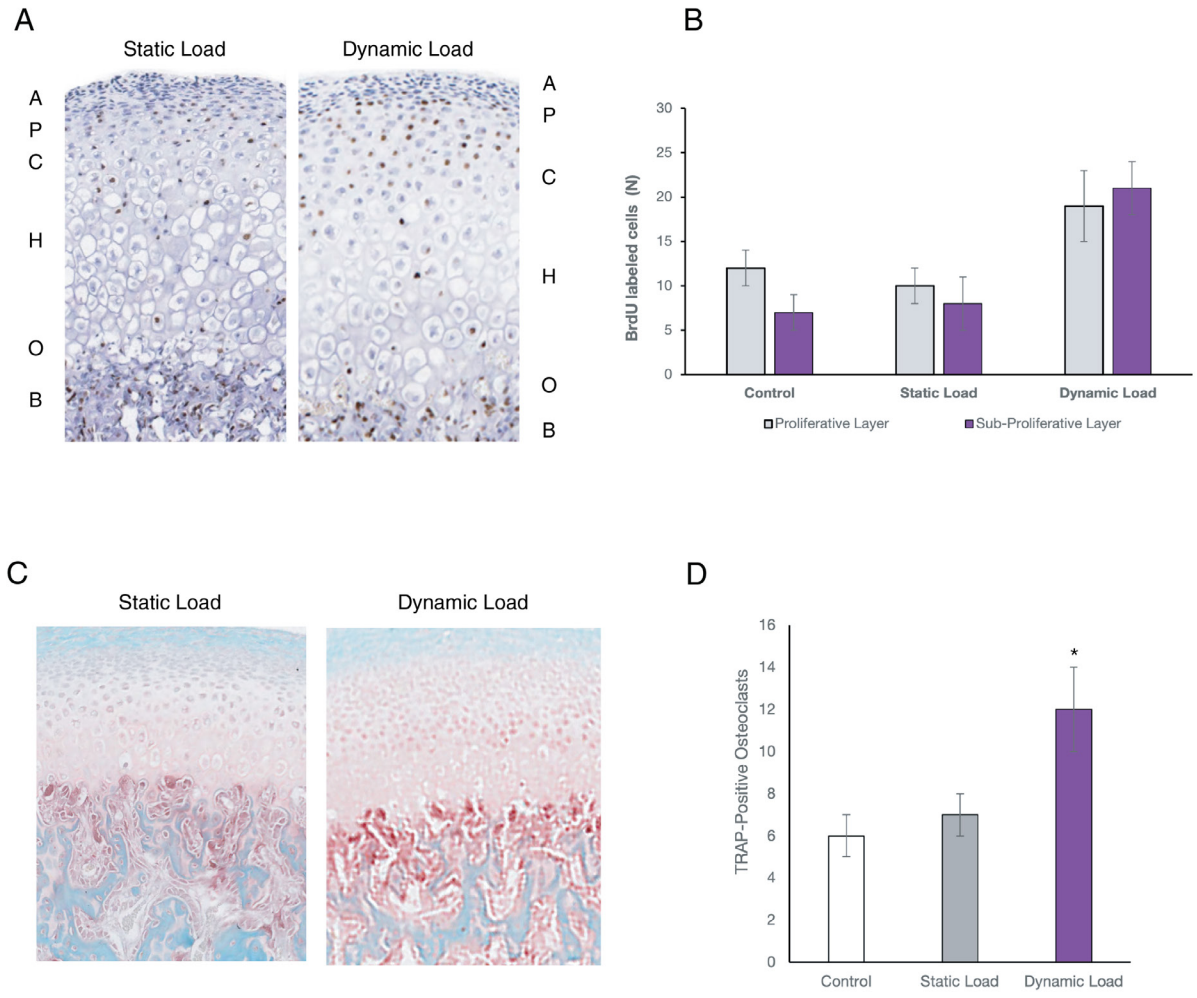

Figure 8: Dynamic loading increases condyle chondrocyte proliferation and osteoclast cell number. *To evaluate the effect of dynamic loading on chondroblast proliferation, BrdU was injected 3 days before euthanasia of the animals. (A) Histological sections from mid-frontal area of condyle were immunostained to identify BrdU-labeled cells. (B) The number of BrdU-labeled cells was significantly higher on both proliferative and sub-proliferative layers (pre-hypertrophic and hypertrophic) in animals that received the dynamic load. BrdU-labeled cells were measured in a fixed rectangular frame in the middle third of mid-frontal condylar sections in 6 consecutive sections. Values are mean ± SEM of 6 animals. (C) To evaluate the effect of dynamic loading on osteoclast activity during endochondral bone formation, frontal sections of condylar cartilage were immunostained for TRAcP-5b and visualized as red cells. (D) The number of osteoclasts was measured in 5 consecutive sections of the middle third of condylar cartilage in a fix frame. Each value presents the mean ± SEM of 6 animals. * Significantly different from Control and Static Load groups.*

In response to indirect dynamic load, expression of transcription factors Sox 9 and Foxo3a, which play important roles in mesenchymal cell differentiation into chondroblasts, increased significantly ($p < 0.01$). Expression of PTHrP and IHH, factors that control the rate of differentiation of chondroblasts and their maturation into hypertrophic cells, also increased significantly ($p < 0.01$). This was accompanied by increased expression of matrix proteins, such as Col2a1 and Col9a1, and Col10a1, which is a marker of the hypertrophic stage ($p < 0.01$). We also measured expression of vascular endothelial growth factor (VEGF; a marker of endochondral bone formation) and the osteoclastic marker RANK. Both genes showed a significant increase in response to dynamic loading ($p < 0.01$; Figure 9A).

Further RNA analysis demonstrated that the expression of osteogenic transcription factors Runx2, Foxo1 and Osterix were all significantly increased in response to indirect dynamic loading ($p < 0.01$; Figure 9B). Similarly, the expression of osteogenic markers ColIa1 and OCN demonstrated a significant increase ($p < 0.01$). To study the pathway through which indirect dynamic loading may trigger chondrogenic or osteogenic differentiation, expression of BMP2 and B-catenin (a key factor in the canonical Wnt pathway) were measured. Indirect dynamic loading significantly upregulated the expression of both molecules ($p < 0.01$;Figure 9B).

No statistical difference was observed in any chondrogenic or osteogenic gene expression between Control and Static groups ($p > 0.05$).

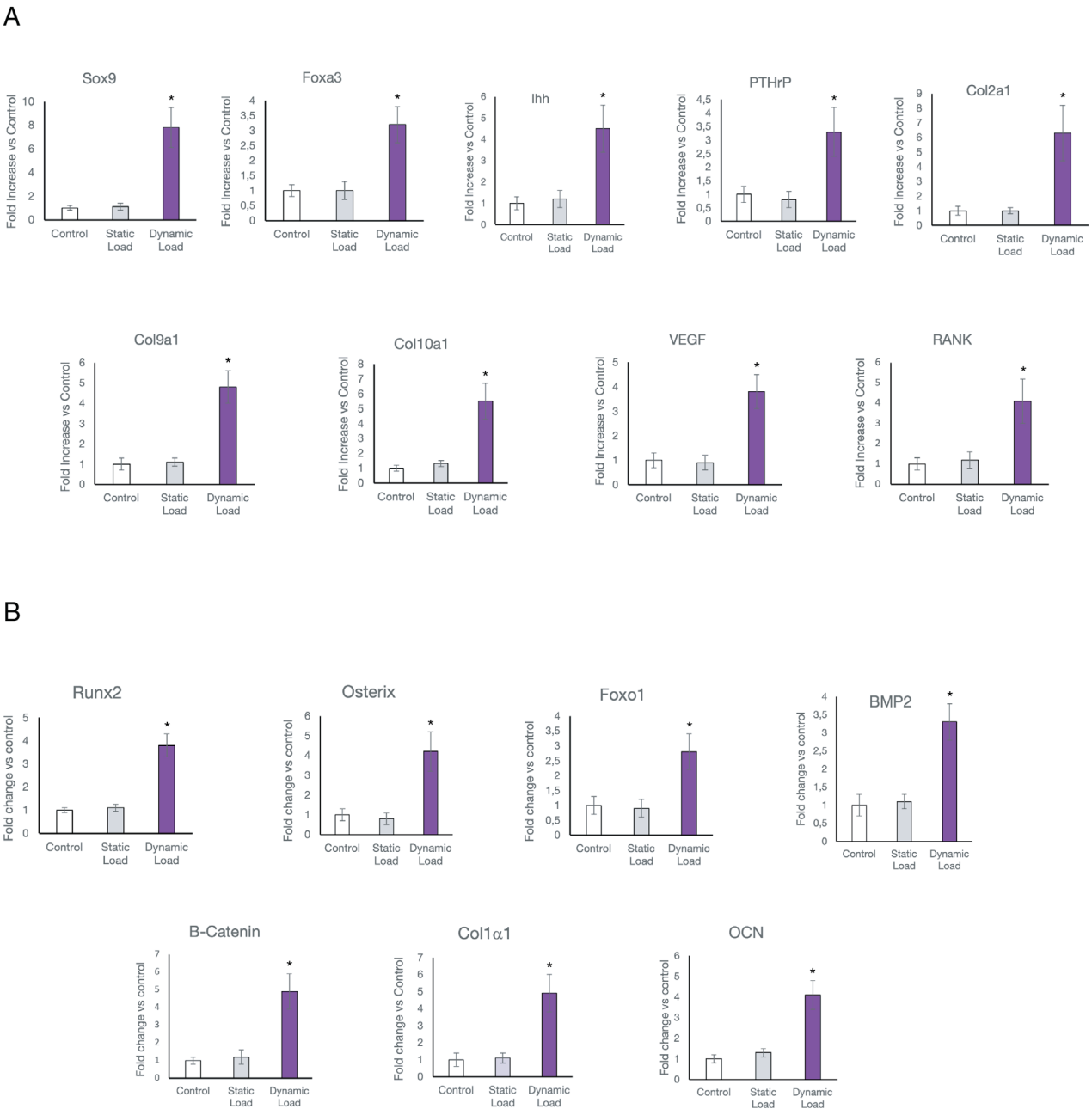

Figure 9: Analysis of chondrogenic and osteogenic markers in response to dynamic loading. *RNA was collected from condyles of animals that received static or dynamic loading for 28 days and the expression of chondrogenic genes (Sox9, Foxa3, Ihh, PTHrP, Col 2α1 Col 9α1, Col 10α1, VEGF), osteoclast marker (RANK) (A), and osteogenic genes (Runx2, Osterix, Foxo1, BMP2, B-Catenin, Col 1α1, OC) (B) was measured by real time RT-PCR. Data are shown as "fold change" in gene expression in comparison to the Control group. Each value presents the mean ± SEM of 3 animals. * Significant different from Control and Static Load groups.*

Discussion

The effect of mechanical stimulation on condylar cartilage has been studied previously [13, 14, 16, 45, 46]; however, it is not clear which component of mechanical stimulation has an anabolic effect and which component has a catabolic effect. This is due to the complexity of the TMJ structure that does not allow isolating the effect of one parameter from others, in vivo. For example, the majority of the studies that apply static loads to the TMJ could not determine if the observed effect is purely the result of the static load's magnitude or alteration of the physiological dynamic load due to the superimposition of the static load. *In vitro* studies and computer modeling studies on the other hand, while they can decrease the number of variables, at best still only model the *in vivo* conditions, and therefore, they should only be used as supplementary studies and not definitive studies [47-50]. In addition, it is very difficult to directly measure mechanical stimulation on the condyle, making these studies technique-dependent. Different researchers may employ different measurement devices or, if using the same device, may not have calibrated the device similar to other researchers. The result of this inconsistent methodology is that these experiments may actually overload or underload the condyle and generate data that do not represent a normal physiological response, instead leading researchers to conclude that loading either has no effect (underloading) or is pathologic (overloading) [51-53].

In the current study, we focused on evaluating the response of condylar cartilage to the local application of low-magnitude, high-frequency dynamic loading. Our study demonstrated that the point of application of the load is very important. We found a significant change in the condyle when the dynamic load was delivered close to the condyle. On the other hand, no significant changes in the condyle were detected when the dynamic load was delivered farther from the condyle. This can explain why our findings do not corroborate previous studies on the lack of an effect of whole-body vibration on condylar cartilage [54-56]. While whole-body vibration has an anabolic effect on weight-bearing bones [21, 27, 28, 54, 57-59], it does not have an anabolic effect on non-weight bearing craniofacial bones [60]. For vibration to be effective on craniofacial bones, it needs to be switched from whole-body vibration (delivered through the feet while standing on vibration plates) to vibration delivered directly to the craniofacial bones. However, due to the damping effect of the soft tissues, the craniofacial bones do not respond to this stimulation. This is especially true for condylar studies, as there is significant skin, muscle and ligament/tendon soft tissue surrounding the condylar bone. Thus, it is reasonable to assume that the condyles also do not receive adequate mechanical stimulation in response to whole body vibration.

Similar to our findings in this study, we have previously reported that when the point of dynamic load application is moved close to the craniofacial structures, a significant anabolic effect of this mechanical stimulation was observed on alveolar bone [29, 30, 61].

The magnitude of the load in our design was very low (30 με) when registered on the buccal bone surrounding the molar teeth on the same side of the stimulated condyle. Applying this magnitude of load as a static load does not have an osteogenic effect on bone [19]. Our study demonstrates that a 5-minute application of static load of equal magnitude as the dynamic load was not able to induce any changes in the condylar cartilage compared to the Control group. This supports the argument that the magnitude of the load cannot explain the changes observed in the condylar cartilage in response to the dynamic load. Therefore, one can attribute the anabolic changes observed here to other parameters of the mechanical stimulation, namely the acceleration and/or frequency. This is in agreement with what has been reported in bone [22, 29]. It should be emphasized that in these experiments the duration of load application was short and the animals were not engaged in any other activity during load application, which decreases the possibility that other factors, other than frequency and acceleration, could affect the results.

The fact that chondrocytes similar to osteoblasts can react to load acceleration and frequency in the absence of matrix deformation was confirmed by *in vitro* data, which demonstrated that both US and LS progenitor cells are sensitive to direct application of low-magnitude, high-frequency dynamic loading, in spite of negligible amount of strain; however, the response was specific to the type of cell or cartilage.

To understand the unique ability of mandibular condylar cartilage to adapt to mechanical stimulation, we should pay attention to its cellular structure. Similar to primary cartilage, cells in the mandibular condylar cartilage are organized into different layers: mesenchymal cells gradually proliferate and differentiate into chondroblasts, which then mature into hypertrophic cells that soon after are replaced by bone through endochondral bone formation [62, 63]. Therefore, mesenchymal cells in the condylar cartilage play a significant role in controlling the magnitude of cartilage formation. This is very important. While in primary cartilage the number of chondroblast progenitor cells for are tightly controlled genetically, in the condyles the ability of mesenchymal cells to differentiate into chondroblasts in response to mechanical stimulation, at least in growing animals, allows for significant adaptability of the shape and size of the condylar cartilage to its mechanical environment [6, 64]. The increase in mesenchymal cell proliferation in our experiment testifies to this adaptability.

Low-magnitude, high-frequency dynamic loading not only affects the proliferation of mesenchymal cells, but also has a great impact on their further differentiation and maturation both in vivo and in vitro. Our results showed increased height of the pre-hypertrophic (chondroblastic) and hypertrophic layers of the condylar cartilage, and the presence of a significant number of BrdU-stained mesenchymal cells in the pre-hypertrophic layer, suggesting an increased rate of progenitor cell differentiation when dynamic loading is delivered. This is in agreement

with previous observations that demonstrate a similar increase in the rate of differentiation in response to mechanical stimulation [65-70]. Our *in vitro* study, however supports the notion that this differentiation was specific to progenitor cells that show maturation ability (US chondrocytes) and can mediate endochondral bone formation, and not immature cells that show articular cartilage characteristics (LS chondrocytes). While these findings agree with previous studies [71], they also help explain the contradictory findings in the literature with regard to different types of cartilage and their different responses to dynamic loading [72, 73].

The mechano-sensitivity observed in mesenchymal cells of the condylar cartilage in response to dynamic loading was similar to the mechano-sensitivity observed in mesenchymal cells that differentiate into osteoblasts in bone [74-82]. This argues that sensitivity to mechanical stimulation is a characteristic of osteo-chondro progenitor cells that is transferred into both osteoprogenitor and chondroprogenitor descendent cells, and later into osteoblasts and chondroblasts. However, local factors in addition to mechanical stimulation, play a role in defining their fate as bone or cartilage cells. Due to this versatility, perhaps some of the mesenchymal cells of the condylar cartilage, especially in places where the periosteum joins the cartilage, may directly differentiate into osteoblasts and contribute to the condylar process remodeling without going through the endochondral bone formation pathway [83]. This possibility can explain bone growth in the posterior area of the condyle that has been reported in some adult patients in response to orthopedic appliances [84].

For mesenchymal cells to differentiate into chondroblasts, Sox9 and Foxo3a transcription factor upregulation is required [85-87] and was observed in our studies in response to dynamic loading. Sox9 regulates the synthesis of type II collagen, the main component of condylar cartilage pericellular and extracellular matrix, thus affecting condylar cartilage formation and, subsequently, condylar growth. The observed increase in Col2a1 and Col9a1 expression and other components of the cartilage matrix [88] also demonstrates active-matrix synthesis in response to dynamic loading. Furthermore, Sox9 upregulation is controlled by parathyroid-hormone-related protein (PTHrP). Our data shows that PTHrP expression was increased in response to dynamic loading. However, PTHrP, in addition to upregulating chondroblast differentiation from mesenchymal cells, delays their maturation to the hypertrophic stage. This is a major regulatory point for continuing condylar growth. This allow the chondrogenesis to continue and the chondrocyte population to increase in the pre-hypertrophic layer as we observed in histological sections. The increase in the expression of PTHrP was accompanied with the increase in expression of Indian hedgehog (Ihh), a protein that is synthesized by pre-hypertrophic and early hypertrophic cells, that is part of a feedback loop controlling chondrocyte differentiation and maturation by regulating PTHrP expression [89, 90]. Expansion of the pre-hypertrophic layer was subsequently followed by the enlargement of the hypertrophic layer. This was confirmed by an increase in the expression of collagen type X (Col10a1), a protein that is expressed exclusively by hypertrophic chondrocytes [90].

Our data showed that the length of the pre-hypertrophic and hypertrophic layers did not change significantly when dynamic load application extended from 28 to 56 days. These findings suggest that, first, since this stimulatory effect was maintained for 56 days, the effect was prolonged and not transitory. Second, the fact that the effect plateaued and no significant increase was observed between 28 and 56 days, demonstrated that the tissues adapted to dynamic stimulation. Longer studies are required to determine if these responses can continue for longer periods of time (more than 56 days) and if changing the frequency and acceleration of applied load can overcome adaptation to stimulation, allowing the therapeutic benefit of dynamic loading to be prolonged over time.

During endochondral ossification, the cartilage template is eventually replaced by bone. VEGF has been show to play an important role not only in endothelial cell recruitment, but also in osteoclast recruitment at the chondro-osseous junction [91, 92]. In our experiments, in response to the application of dynamic loading, expression of both VEGF and RANK (osteoclast marker) increased, and subsequently osteoclast numbers increased. VEGF-induced vascular invasion and osteoclast recruitment and activation is viewed as an early step in the replacement of a mineralized cartilage with bone. A second and equally important step on this process is the differentiation of mesenchymal cells into osteoblasts, which then deposit the first osteoid. We did find an initial expression of the osteogenic transcription factors such as Foxo1, Runx2, and Osterix, which play a role in mesenchymal cell differentiation into the osteoblast lineage [93-95]. This increase was accompanied by expression of the early osteoblast differentiation marker type I collagen (Col1a1) and late osteoblast differentiation marker osteocalcin (OC) [96, 97].

As discussed earlier, dynamic loading may direct mesenchymal cells toward osteogenic or chondrogenic pathways. But how this direct stimulation is regulated at the molecular level is not fully understood. One possibility is through the activation of the Wnt pathway. Wnts are a family of secreted proteins extensively expressed within the skeleton that bind to membrane-bound Frizzled and Lrp5/6 co-receptors. When activated, Frizzled and Lrp 5/6 receptors stabilize B-catenin in the cytoplasm, which then upregulates the expression of osteogenic or chondrogenic markers [98-101]. Our results showed that the expression of B-catenin increased significantly in response to dynamic loading. In addition, we also observed an increase in BMP2 expression, which could also mediate the effect of dynamic loading on the differentiation of mesenchymal cells along chondrogenic or osteogenic pathways. It should be emphasized all these factors, BMP2, Runx2, and B-catenin, play a role in both bone and cartilage differentiation. Therefore, future studies are required to dissect the roles of

different pathways in mediating the chondrogenic or osteogenic effects of dynamic loading.

Dynamic loading was accompanied with a striking increase in bone volume fraction, bone mineral density and trabecular thickness. In view of the discussion above, the interpretation of these data should be done cautiously since this adaptation can be both due to the direct effect of dynamic loading on existing sub-condylar bone (we and others have shown that bone formation increase in response to dynamic loading [29, 30, 61]) and to an increase in the rate of endochondral bone formation.

All of the changes reported here, ultimately manifest themselves as an increase in the length of the condylar process. Based on these data, dynamic loading by itself may not be enough stimulation for treatment of a mandibular deficiency. The increase in the condylar process length is small and could be easily compensated or obscured by changes in morphology of the other components of the mandible, such as an increase in curvature of the ramus, as it was observed here. However, in the presence of orthopedic appliances that aim to stimulate the sagittal growth of the mandible, dynamic loading could support and amplify the effect of treatment significantly. Current studies at our research center are looking at this combined effect.

Conclusion

As a mechanosensitive tissue, condylar cartilage adapts its cellular responses and microstructure in response to dynamic loading by different mechanisms:

1. Increased mesenchymal cell proliferation and chondrogenic differentiation resulting in increased height of pre-hypertrophic (chondroblast) and hypertrophic layers
2. Increase in expression of both chondrogenic and osteogenic markers
3. Increased endochondral bone formation and bone density of the condylar process
4. Increase in condylar process length

Our studies show that low-magnitude, high-frequency dynamic loading has the potential to stimulate condylar cartilage and endochondral bone formation, and therefore enhance or facilitate correction of mandibular deficiency when combined with orthopedic appliances.

.

References

1. Grodzinsky AJ, Levenston ME, Jin M, Frank EH. Cartilage tissue remodeling in response to mechanical forces. Annu Rev Biomed Eng. 2000;2:691-713. doi: 10.1146/annurev.bioeng.2.1.691. PubMed PMID: 11701528.

2. Mizuno E, Wakimoto Y, Nomura M, Kohara Y, Shimaya S, Suzuki R, et al. Effects of different exercises on the growth plate in young growing mice. Biomedical Research (0970-938X). 2018;29(12).

3. Villemure I, Stokes IA. Growth plate mechanics and mechanobiology. A survey of present understanding. J Biomech. 2009;42(12):1793-803. Epub 20090621. doi: 10.1016/j.jbiomech.2009.05.021. PubMed PMID: 19540500; PubMed Central PMCID: PMCPMC2739053.

4. Solem RC, Eames BF, Tokita M, Schneider RA. Mesenchymal and mechanical mechanisms of secondary cartilage induction. Dev Biol. 2011;356(1):28-39. Epub 20110511. doi: 10.1016/j.ydbio.2011.05.003. PubMed PMID: 21600197; PubMed Central PMCID: PMCPMC3130809.

5. Merida Velasco JR, Rodriguez Vazquez JF, De la Cuadra Blanco C, Campos Lopez R, Sanchez M, Merida Velasco JA. Development of the mandibular condylar cartilage in human specimens of 10-15 weeks' gestation. J Anat. 2009;214(1):56-64. doi: 10.1111/j.1469-7580.2008.01009.x. PubMed PMID: 19166473; PubMed Central PMCID: PMCPMC2667917.

6. Delatte M, Von den Hoff JW, Van Rheden REM, Kuijpers-Jagtman AM. Primary and secondary cartilages of the neonatal rat: the femoral head and the mandibular condyle. European Journal of Oral Sciences. 2004;112(2):156-62. doi: https://doi.org/10.1111/j.0909-8836.2004.00108.x.

7. Shen G, Darendeliler MA. The adaptive remodeling of condylar cartilage---a transition from chondrogenesis to osteogenesis. J Dent Res. 2005;84(8):691-9. doi: 10.1177/154405910508400802. PubMed PMID: 16040724.

8. Baume LJ, Derichsweiler H. Response of Condylar Growth Cartilage to Induced Stresses. Science. 1961;134(3471):53-4. doi: doi:10.1126/science.134.3471.53.

9. Moss ML, Salentijn L. The primary role of functional matrices in facial growth. Am J Orthod. 1969;55(6):566-77. doi: 10.1016/0002-9416(69)90034-7. PubMed PMID: 5253955.

10. Moss ML, Salentijn L. The capsular matrix. Am J Orthod. 1969;56(5):474-90. doi: 10.1016/0002-9416(69)90209-7. PubMed PMID: 5261161.

11. Enlow DH, Harris DB. A study of the postnatal growth of the human mandible. American Journal of Orthodontics. 1964;50(1):25-50. doi: https://doi.org/10.1016/S0002-9416(64)80016-6.

12. Kantomaa T, Tuominen M, Pirttiniemi P. Effect of mechanical forces on chondrocyte maturation and differentiation in the mandibular condyle of the rat. J Dent Res. 1994;73(6):1150-6. doi: 10.1177/00220345940730060401. PubMed PMID: 8046103.

13. Utreja A, Dyment NA, Yadav S, Villa MM, Li Y, Jiang X, et al. Cell and matrix response of temporomandibular cartilage to mechanical loading. Osteoarthritis Cartilage. 2016;24(2):335-44. Epub 20150908. doi: 10.1016/j.joca.2015.08.010. PubMed PMID: 26362410; PubMed Central PMCID: PMCPMC4757844.

14. Kaul R, O'Brien MH, Dutra E, Lima A, Utreja A, Yadav S. The Effect of Altered Loading on Mandibular Condylar Cartilage. PLOS ONE. 2016;11(7):e0160121. doi: 10.1371/journal.pone.0160121.

15. Teramoto M, Kaneko S, Shibata S, Yanagishita M, Soma K. Effect of compressive forces on extracellular matrix in rat mandibular condylar cartilage. J Bone Miner Metab. 2003;21(5):276-86. doi: 10.1007/s00774-003-0421-y. PubMed PMID: 12928828.

16. Kuroda S, Tanimoto K, Izawa T, Fujihara S, Koolstra JH, Tanaka E. Biomechanical and biochemical characteristics of the mandibular condylar cartilage. Osteoarthritis Cartilage. 2009;17(11):1408-15. Epub 20090518. doi: 10.1016/j.joca.2009.04.025. PubMed PMID: 19477310.

17. Bouvier M, Hylander WL. The effect of dietary consistency on gross and histologic morphology in the craniofacial region of young rats. American Journal of Anatomy. 1984;170(1):117-26. doi: https://doi.org/10.1002/aja.1001700109.

18. Hinton RJ, Carlson DS. Response of the mandibular joint to loss of incisal function in the rat. Acta Anat (Basel). 1986;125(3):145-51. doi: 10.1159/000146153. PubMed PMID: 3962576.

19. Turner CH, Forwood MR, Rho JY, Yoshikawa T. Mechanical loading thresholds for lamellar and woven bone formation. J Bone Miner Res. 1994;9(1):87-97. doi: 10.1002/jbmr.5650090113. PubMed PMID: 8154314.

20. Oxlund BS, Ørtoft G, Andreassen TT, Oxlund H. Low-intensity, high-frequency vibration appears to prevent the decrease in strength of the femur

and tibia associated with ovariectomy of adult rats. Bone. 2003;32(1):69-77. doi: https://doi.org/10.1016/S8756-3282(02)00916-X.

21. Rubin C, Turner AS, Bain S, Mallinckrodt C, McLeod K. Anabolism. Low mechanical signals strengthen long bones. Nature. 2001;412(6847):603-4. doi: 10.1038/35088122. PubMed PMID: 11493908.

22. Garman R, Gaudette G, Donahue LR, Rubin C, Judex S. Low-level accelerations applied in the absence of weight bearing can enhance trabecular bone formation. J Orthop Res. 2007;25(6):732-40. doi: 10.1002/jor.20354. PubMed PMID: 17318899.

23. Rubin CT, Lanyon LE. Regulation of bone mass by mechanical strain magnitude. Calcif Tissue Int. 1985;37(4):411-7. doi: 10.1007/bf02553711. PubMed PMID: 3930039.

24. Li Y, Frank EH, Wang Y, Chubinskaya S, Huang HH, Grodzinsky AJ. Moderate dynamic compression inhibits pro-catabolic response of cartilage to mechanical injury, tumor necrosis factor-α and interleukin-6, but accentuates degradation above a strain threshold. Osteoarthritis Cartilage. 2013;21(12):1933-41. Epub 20130903. doi: 10.1016/j.joca.2013.08.021. PubMed PMID: 24007885; PubMed Central PMCID: PMCPMC3855909.

25. Frost HM. Review article mechanical determinants of bone modeling. Metabolic Bone Disease and Related Research. 1982;4(4):217-29. doi: https://doi.org/10.1016/0221-8747(82)90031-5.

26. Tägil M, Aspenberg P. Cartilage induction by controlled mechanical stimulation in vivo. Journal of Orthopaedic Research. 1999;17(2):200-4. doi: https://doi.org/10.1002/jor.1100170208.

27. von Stengel S, Kemmler W, Engelke K, Kalender WA. Effects of whole body vibration on bone mineral density and falls: results of the randomized controlled ELVIS study with postmenopausal women. Osteoporos Int. 2011;22(1):317-25. Epub 20100320. doi: 10.1007/s00198-010-1215-4. PubMed PMID: 20306017.

28. Zhou Y, Guan X, Liu T, Wang X, Yu M, Yang G, et al. Whole body vibration improves osseointegration by up-regulating osteoblastic activity but down-regulating osteoblast-mediated osteoclastogenesis via ERK1/2 pathway. Bone. 2015;71:17-24. Epub 20141007. doi: 10.1016/j.bone.2014.09.026. PubMed PMID: 25304090.

29. Alikhani M, Khoo E, Alyami B, Raptis M, Salgueiro JM, Oliveira SM, et al. Osteogenic Effect of High-frequency Acceleration on Alveolar Bone. Journal of Dental Research. 2012;91(4):413-9. doi: 10.1177/0022034512438590. PubMed PMID: 22337699.

30. Alikhani M, Lopez JA, Alabdullah H, Vongthongleur T, Sangsuwon C, Alikhani M, et al. High-Frequency Acceleration:Therapeutic Tool to Preserve Bone following Tooth Extractions. Journal of Dental Research. 2016;95(3):311-8. doi: 10.1177/0022034515621495. PubMed PMID: 26672126.

31. Goldring MB, Tsuchimochi K, Ijiri K. The control of chondrogenesis. J Cell Biochem. 2006;97(1):33-44. doi: 10.1002/jcb.20652. PubMed PMID: 16215986.

32. Iwamoto M, Shapiro IM, Yagami K, Boskey AL, Leboy PS, Adams SL, et al. Retinoic acid induces rapid mineralization and expression of mineralization-related genes in chondrocytes. Exp Cell Res. 1993;207(2):413-20. doi: 10.1006/excr.1993.1209. PubMed PMID: 8344389.

33. Oliveira SM, Turner G, Rodrigues SP, Barbosa MrA, Alikhani M, Teixeira CC. Spontaneous Chondrocyte Maturation on 3D-Chitosan Scaffolds. Journal of Tissue Science and Engineering. 2013;2013.

34. Judex S, Pongkitwitoon S. Differential Efficacy of 2 Vibrating Orthodontic Devices to Alter the Cellular Response in Osteoblasts, Fibroblasts, and Osteoclasts. Dose Response. 2018;16(3):1559325818792112. Epub 20180816. doi: 10.1177/1559325818792112. PubMed PMID: 30397398; PubMed Central PMCID: PMCPMC6207979.

35. Teixeira CC, Hatori M, Leboy PS, Pacifici M, Shapiro IM. A rapid and ultrasensitive method for measurement of DNA, calcium and protein content, and alkaline phosphatase activity of chondrocyte cultures. Calcif Tissue Int. 1995;56(3):252-6. doi: 10.1007/BF00298620. PubMed PMID: 7538446.

36. Leboy PS, Vaias L, Uschmann B, Golub E, Adams SL, Pacifici M. Ascorbic acid induces alkaline phosphatase, type X collagen, and calcium deposition in cultured chick chondrocytes. J Biol Chem. 1989;264(29):17281-6. PubMed PMID: 2793855.

37. Teixeira CC, Costas AP, Nemelivsky Y. Apoptosis of growth plate chondrocytes occurs through a mitochondrial pathway. Angle Orthod. 2007;77(1):129-34. doi: 10.2319/062805-210R.1. PubMed PMID: 17029540.

38. Teixeira CC, Mansfield K, Hertkorn C, Ischiropoulos H, Shapiro IM. Phosphate-induced chondrocyte apoptosis is linked to nitric oxide generation. Am J Physiol Cell Physiol. 2001;281(3):C833-9. doi: 10.1152/ajpcell.2001.281.3.C833. PubMed PMID: 11502560.

39. Mosmann T. Rapid colorimetric assay for cellular growth and survival: application to proliferation and cytotoxicity assays. J Immunol Methods. 1983;65(1-2):55-63. doi: 10.1016/0022-1759(83)90303-4. PubMed PMID: 6606682.

40. van de Loosdrecht AA, Beelen RH, Ossenkoppele GJ, Broekhoven MG, Langenhuijsen MM. A tetrazolium-based colorimetric MTT assay to quantitate human monocyte mediated cytotoxicity against leukemic cells from cell lines and patients with acute myeloid leukemia. J Immunol Methods. 1994;174(1-2):311-20. doi: 10.1016/0022-1759(94)90034-5. PubMed PMID: 8083535.

41. Teixeira CC, Khoo E, Tran J, Chartres I, Liu Y, Thant LM, et al. Cytokine expression and accelerated tooth movement. J Dent Res. 2010;89(10):1135-41. Epub 2010/07/20. doi: 10.1177/0022034510373764. PubMed PMID: 20639508; PubMed Central PMCID: PMCPMC3318047.

42. Oliveira SM, Amaral IF, Barbosa MA, Teixeira CC. Engineering endochondral bone: in vitro studies. Tissue Eng Part A. 2009;15(3):625-34. doi: 10.1089/ten.tea.2008.0051. PubMed PMID: 18759672; PubMed Central PMCID: PMCPMC2744199.

43. Oliveira SM, Mijares DQ, Turner G, Amaral IF, Barbosa MA, Teixeira CC. Engineering endochondral bone: in vivo studies. Tissue Eng Part A. 2009;15(3):635-43. doi: 10.1089/ten.tea.2008.0052. PubMed PMID: 18759673; PubMed Central PMCID: PMCPMC2751848.

44. Kumar P, Nagarajan A, Uchil PD. Analysis of Cell Viability by the MTT Assay. Cold Spring Harb Protoc. 2018;2018(6). Epub 20180601. doi: 10.1101/pdb.prot095505. PubMed PMID: 29858338.

45. Sobue T, Yeh W-C, Chhibber A, Utreja A, Diaz-Doran V, Adams D, et al. Murine TMJ Loading Causes Increased Proliferation and Chondrocyte Maturation. Journal of Dental Research. 2011;90(4):512-6. doi: 10.1177/0022034510390810. PubMed PMID: 21248355.

46. Pirttiniemi P, Kantomaa T, Sorsa T. Effect of decreased loading on the metabolic activity of the mandibular condylar cartilage in the rat. Eur J Orthod. 2004;26(1):1-5. doi: 10.1093/ejo/26.1.1. PubMed PMID: 14994876.

47. Li Z, Kupcsik L, Yao SJ, Alini M, Stoddart MJ. Mechanical load modulates chondrogenesis of human mesenchymal stem cells through the TGF-beta pathway. J Cell Mol Med. 2010;14(6a):1338-46. Epub 20090511. doi: 10.1111/j.1582-4934.2009.00780.x. PubMed PMID: 19432813; PubMed Central PMCID: PMCPMC3828850.

48. Trepczik B, Lienau J, Schell H, Epari DR, Thompson MS, Hoffmann JE, et al. Endochondral ossification in vitro is influenced by mechanical bending. Bone. 2007;40(3):597-603. Epub 20061130. doi: 10.1016/j.bone.2006.10.011. PubMed PMID: 17141595.

49. Smith DM, McLachlan KR, McCall WD, Jr. A numerical model of temporomandibular joint loading. J Dent Res. 1986;65(8):1046-52. doi: 10.1177/00220345860650080201. PubMed PMID: 3461020.

50. Koolstra JH, van Eijden TM. The jaw open-close movements predicted by biomechanical modelling. J Biomech. 1997;30(9):943-50. doi: 10.1016/

s0021-9290(97)00058-4. PubMed PMID: 9302617.
51.Ikeda Y, Yonemitsu I, Takei M, Shibata S, Ono T. Mechanical loading leads to osteoarthritis-like changes in the hypofunctional temporomandibular joint in rats. Archives of Oral Biology. 2014;59(12):1368-76. doi: https://doi.org/10.1016/j.archoralbio.2014.08.010.

52. Tanaka E, Koolstra JH. Biomechanics of the Temporomandibular Joint. Journal of Dental Research. 2008;87(11):989-91. doi: 10.1177/154405910808701101. PubMed PMID: 18946004.

53. Walker CG, Ito Y, Dangaria S, Luan X, Diekwisch TG. RANKL, osteopontin, and osteoclast homeostasis in a hyperocclusion mouse model. Eur J Oral Sci. 2008;116(4):312-8. doi: 10.1111/j.1600-0722.2008.00545.x. PubMed PMID: 18705798; PubMed Central PMCID: PMCPMC2597431.

54. Prisby RD, Lafage-Proust MH, Malaval L, Belli A, Vico L. Effects of whole body vibration on the skeleton and other organ systems in man and animal models: what we know and what we need to know. Ageing Res Rev. 2008;7(4):319-29. Epub 20080812. doi: 10.1016/j.arr.2008.07.004. PubMed PMID: 18762281.

55. Sriram D, Jones A, Alatli-Burt I, Darendeliler MA. Effects of mechanical stimuli on adaptive remodeling of condylar cartilage. J Dent Res. 2009;88(5):466-70. doi: 10.1177/0022034509336616. PubMed PMID: 19493892.

56. Fujita T, Hayashi H, Shirakura M, Tsuka Y, Fujii E, Kawata T, et al. Regeneration of condyle with a functional appliance. J Dent Res. 2013;92(4):322-8. Epub 20130225. doi: 10.1177/0022034513480795. PubMed PMID: 23439718.

57. Wysocki A, Butler M, Shamliyan T, Kane RL. Whole-Body Vibration Therapy for Osteoporosis: State of the Science. Annals of Internal Medicine. 2011;155(10):680-6. doi: 10.7326/0003-4819-155-10-201111150-00006 %m 22084334.

58. Totosy de Zepetnek JO, Giangregorio LM, Craven BC. Whole-body vibration as potential intervention for people with low bone mineral density and osteoporosis: a review. J Rehabil Res Dev. 2009;46(4):529-42. doi: 10.1682/jrrd.2008.09.0136. PubMed PMID: 19882487.

59. Xie L, Jacobson JM, Choi ES, Busa B, Donahue LR, Miller LM, et al. Low-level mechanical vibrations can influence bone resorption and bone formation in the growing skeleton. Bone. 2006;39(5):1059-66. Epub 20060707. doi: 10.1016/j.bone.2006.05.012. PubMed PMID: 16824816.

60. Yang P, Jia B, Ding C, Wang Z, Qian A, Shang P. Whole-body vibration effects on bone before and after hind-limb unloading in rats. Aviat Space Environ Med. 2009;80(2):88-93. doi: 10.3357/asem.2368.2009. PubMed PMID: 19198193.

61. Alikhani M, Alikhani M, Alansari S, Almansour A, Hamidaddin MA, Khoo E, et al. Therapeutic effect of localized vibration on alveolar bone of osteoporotic rats. PLoS One. 2019;14(1):e0211004. Epub 20190129. doi: 10.1371/journal.pone.0211004. PubMed PMID: 30695073; PubMed Central PMCID: PMCPMC6350965.

62. Ben-Ami Y, Lewinson D, Silbermann M. Structural characterization of the mandibular condyle in human fetuses: light and electron microscopy studies. Acta Anat (Basel). 1992;145(1):79-87. doi: 10.1159/000147346. PubMed PMID: 1414216.

63. Hinton RJ, Carlson DS. Regulation of Growth in Mandibular Condylar Cartilage. Seminars in Orthodontics. 2005;11(4):209-18. doi: 10.1053/j.sodo.2005.07.005.

64. Copray JC, Jansen HW, Duterloo HS. Growth and growth pressure of mandibular condylar and some primary cartilages of the rat in vitro. Am J Orthod Dentofacial Orthop. 1986;90(1):19-28. doi: 10.1016/0889-5406(86)90023-5. PubMed PMID: 3460343.

65. Rabie AB, Tang GH, Xiong H, Hägg U. PTHrP regulates chondrocyte maturation in condylar cartilage. J Dent Res. 2003;82(8):627-31. doi: 10.1177/154405910308200811. PubMed PMID: 12885848.

66. Lane Smith R, Trindade MC, Ikenoue T, Mohtai M, Das P, Carter DR, et al. Effects of shear stress on articular chondrocyte metabolism. Biorheology. 2000;37(1-2):95-107. PubMed PMID: 10912182.

67. Lee DA, Bader DL. Compressive strains at physiological frequencies influence the metabolism of chondrocytes seeded in agarose. J Orthop Res. 1997;15(2):181-8. doi: 10.1002/jor.1100150205. PubMed PMID: 9167619.

68. Shelton JC, Bader DL, Lee DA. Mechanical conditioning influences the metabolic response of cell-seeded constructs. Cells Tissues Organs. 2003;175(3):140-50. doi: 10.1159/000074630. PubMed PMID: 14663157.

69. Copray JC, Jansen HW, Duterloo HS. Effects of compressive forces on proliferation and matrix synthesis in mandibular condylar cartilage of the rat in vitro. Arch Oral Biol. 1985;30(4):299-304. doi: 10.1016/0003-9969(85)90001-9. PubMed PMID: 3857899.

70. Yang X, Vezeridis PS, Nicholas B, Crisco JJ, Moore DC, Chen Q. Differential expression of type X collagen in a mechanically active 3-D chondrocyte culture system: a quantitative study. J Orthop Surg Res. 2006;1:15. Epub 20061206. doi: 10.1186/1749-799x-1-15. PubMed PMID: 17150098; PubMed Central PMCID: PMCPMC1764003.

71. Elder SH, Goldstein SA, Kimura JH, Soslowsky LJ, Spengler DM. Chondrocyte Differentiation is Modulated by Frequency and Duration of Cyclic Compressive Loading. Annals of Biomedical Engineering. 2001;29(6):476-82. doi: 10.1114/1.1376696.

72. Junbo W, Sijia L, Hongying C, Lei L, Pu W. Effect of low-magnitude different-frequency whole-body vibration on subchondral trabecular bone microarchitecture, cartilage degradation, bone/cartilage turnover, and joint pain in rabbits with knee osteoarthritis. BMC Musculoskeletal Disorders. 2017;18(1):260. doi: 10.1186/s12891-017-1579-0.

73. McCann MR, Yeung C, Pest MA, Ratneswaran A, Pollmann SI, Holdsworth DW, et al. Whole-body vibration of mice induces articular cartilage degeneration with minimal changes in subchondral bone. Osteoarthritis and Cartilage. 2017;25(5):770-8. doi: https://doi.org/10.1016/j.joca.2016.11.001.

74. Tirkkonen L, Halonen H, Hyttinen J, Kuokkanen H, Sievänen H, Koivisto A-M, et al. The effects of vibration loading on adipose stem cell number, viability and differentiation towards bone-forming cells. Journal of the Royal Society, Interface. 2011;8(65):1736-47. Epub 2011/05/25. doi: 10.1098/rsif.2011.0211. PubMed PMID: 21613288.

75. Kim IS, Song YM, Lee B, Hwang SJ. Human Mesenchymal Stromal Cells are Mechanosensitive to Vibration Stimuli. Journal of Dental Research. 2012;91(12):1135-40. doi: 10.1177/0022034512465291. PubMed PMID: 23086742.

76. Zhang C, Li J, Zhang L, Zhou Y, Hou W, Quan H, et al. Effects of mechanical vibration on proliferation and osteogenic differentiation of human periodontal ligament stem cells. Archives of Oral Biology. 2012;57(10):1395-407. doi: https://doi.org/10.1016/j.archoralbio.2012.04.010.

77. Prè D, Ceccarelli G, Visai L, Benedetti L, Imbriani M, De Angelis MC, et al. High-frequency vibration treatment of human bone marrow stromal cells increases differentiation toward bone tissue. Bone marrow research. 2013;2013.

78. Uzer G, Pongkitwitoon S, Ete Chan M, Judex S. Vibration induced osteogenic commitment of mesenchymal stem cells is enhanced by cytoskeletal remodeling but not fluid shear. Journal of Biomechanics. 2013;46(13):2296-302. doi: https://doi.org/10.1016/j.jbiomech.2013.06.008.

79. Chen X, He F, Zhong D-Y, Luo Z-P. Acoustic-frequency vibratory stimulation regulates the balance between osteogenesis and adipogenesis of human bone marrow-derived mesenchymal stem cells. BioMed research international. 2015;2015.

80. Pongkitwitoon S, Uzer G, Rubin J, Judex S. Cytoskeletal Configuration Modulates Mechanically Induced Changes in Mesenchymal Stem Cell Osteogenesis, Morphology, and Stiffness. Scientific Reports. 2016;6(1):34791.

doi: 10.1038/srep34791.
81. Marędziak M, Lewandowski D, Tomaszewski KA, Kubiak K, Marycz K. The Effect of Low-Magnitude Low-Frequency Vibrations (LMLF) on Osteogenic Differentiation Potential of Human Adipose Derived Mesenchymal Stem Cells. Cellular and Molecular Bioengineering. 2017;10(6):549-62. doi: 10.1007/s12195-017-0501-z.

82. Lu Y, Zhao Q, Liu Y, Zhang L, Li D, Zhu Z, et al. Vibration loading promotes osteogenic differentiation of bone marrow-derived mesenchymal stem cells via p38 MAPK signaling pathway. Journal of Biomechanics. 2018;71:67-75. doi: https://doi.org/10.1016/j.jbiomech.2018.01.039.

83. Dean D. Facial growth, 3rd ed. By D. H. Enlow. Philadelphia: W. B. Saunders. 1990. 576 pp. $79.00 (cloth). American Journal of Physical Anthropology. 1991;86(1):90-2. doi: https://doi.org/10.1002/ajpa.1330860111.

84. Paulsen HU. Morphological changes of the TMJ condyles of 100 patients treated with the Herbst appliance in the period of puberty to adulthood: A long-term radiographic study. European Journal of Orthodontics. 1997;19(6):657-68. doi: 10.1093/ejo/19.6.657.

85. Nishimura R, Hata K, Takahata Y, Murakami T, Nakamura E, Yagi H. Regulation of Cartilage Development and Diseases by Transcription Factors. jbm. 2017;24(3):147-53. doi: 10.11005/jbm.2017.24.3.147.

86. Bielajew BJ, Hu JC, Athanasiou KA. Collagen: quantification, biomechanics and role of minor subtypes in cartilage. Nature Reviews Materials. 2020;5(10):730-47. doi: 10.1038/s41578-020-0213-1.

87. Djouad F, Bony C, Canovas F, Fromigué O, Rème T, Jorgensen C, et al. Transcriptomic analysis identifies Foxo3A as a novel transcription factor regulating mesenchymal stem cell chrondrogenic differentiation. Cloning Stem Cells. 2009;11(3):407-16. doi: 10.1089/clo.2009.0013. PubMed PMID: 19751111.

88. Olsen BR. Collagen IX. Int J Biochem Cell Biol. 1997;29(4):555-8. doi: 10.1016/s1357-2725(96)00100-8. PubMed PMID: 9363632.

89. Kronenberg HM. Developmental regulation of the growth plate. Nature. 2003;423(6937):332-6. doi: 10.1038/nature01657.

90. Shibukawa Y, Young B, Wu C, Yamada S, Long F, Pacifici M, et al. Temporomandibular joint formation and condyle growth require Indian hedgehog signaling. Dev Dyn. 2007;236(2):426-34. doi: 10.1002/dvdy.21036. PubMed PMID: 17191253.

91. Carlevaro MF, Cermelli S, Cancedda R, Descalzi Cancedda F. Vascular endothelial growth factor (VEGF) in cartilage neovascularization and chondrocyte differentiation: auto-paracrine role during endochondral bone formation. Journal of Cell Science. 2000;113(1):59-69. doi: 10.1242/jcs.113.1.59.

92. Gerber HP, Vu TH, Ryan AM, Kowalski J, Werb Z, Ferrara N. VEGF couples hypertrophic cartilage remodeling, ossification and angiogenesis during endochondral bone formation. Nat Med. 1999;5(6):623-8. doi: 10.1038/9467. PubMed PMID: 10371499.

93. Komori T. Regulation of osteoblast differentiation by transcription factors. Journal of Cellular Biochemistry. 2006;99(5):1233-9. doi: https://doi.org/10.1002/jcb.20958.

94. Nakashima K, Zhou X, Kunkel G, Zhang Z, Deng JM, Behringer RR, et al. The novel zinc finger-containing transcription factor osterix is required for osteoblast differentiation and bone formation. Cell. 2002;108(1):17-29. doi: 10.1016/s0092-8674(01)00622-5. PubMed PMID: 11792318.

95. Teixeira CC, Liu Y, Thant LM, Pang J, Palmer G, Alikhani M. Foxo1, a novel regulator of osteoblast differentiation and skeletogenesis. J Biol Chem. 2010;285(40):31055-65. Epub 20100722. doi: 10.1074/jbc.M109.079962. PubMed PMID: 20650891; PubMed Central PMCID: PMCPMC2945596.

96. Ota T, Chiba M, Hayashi H. Vibrational stimulation induces osteoblast differentiation and the upregulation of osteogenic gene expression in vitro. Cytotechnology. 2016;68(6):2287-99. doi: 10.1007/s10616-016-0023-x.
97. Stein GS, Lian JB. Molecular mechanisms mediating proliferation/differentiation interrelationships during progressive development of the osteoblast phenotype. Endocr Rev. 1993;14(4):424-42. doi: 10.1210/edrv-14-4-424. PubMed PMID: 8223340.

98. Krishnan V, Bryant HU, Macdougald OA. Regulation of bone mass by Wnt signaling. J Clin Invest. 2006;116(5):1202-9. doi: 10.1172/jci28551. PubMed PMID: 16670761; PubMed Central PMCID: PMCPMC1451219.

99. Baron R, Kneissel M. WNT signaling in bone homeostasis and disease: from human mutations to treatments. Nature Medicine. 2013;19(2):179-92. doi: 10.1038/nm.3074.

100. Dao DY, Jonason JH, Zhang Y, Hsu W, Chen D, Hilton MJ, et al. Cartilage-specific β-catenin signaling regulates chondrocyte maturation, generation of ossification centers, and perichondrial bone formation during skeletal development. Journal of Bone and Mineral Research. 2012;27(8):1680-94. doi: https://doi.org/10.1002/jbmr.1639.

101. Golovchenko S, Hattori T, Hartmann C, Gebhardt M, Gebhard S, Hess A, et al. Deletion of beta catenin in hypertrophic growth plate chondrocytes impairs trabecular bone formation. Bone. 2013;55(1):102-12. doi: https://doi.org/10.1016/j.bone.2013.03.019.